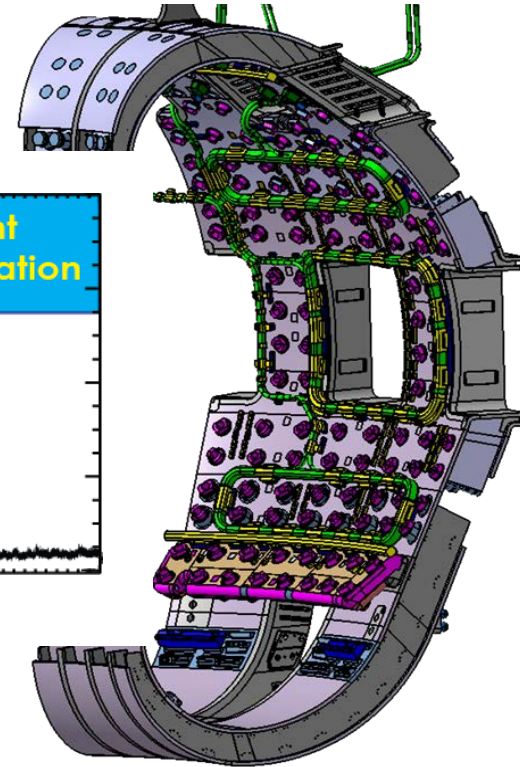
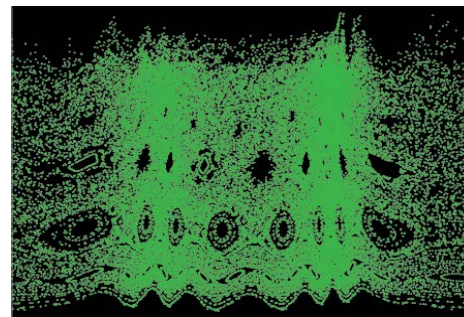
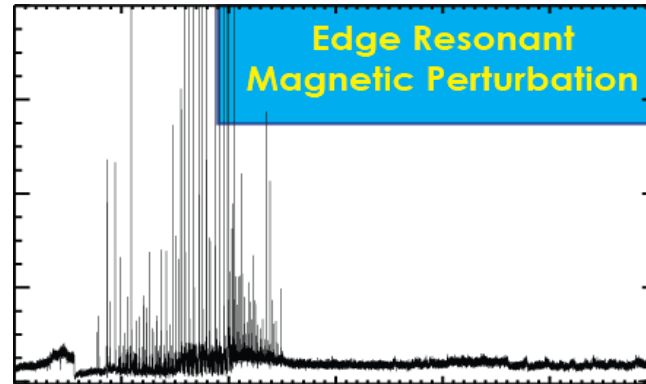
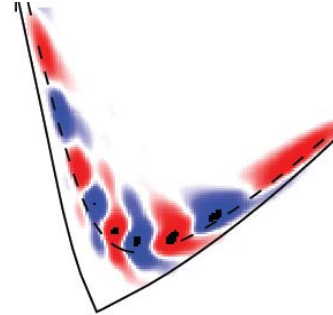


Advances in the Physics Understanding of ELM Suppression Using Resonant Magnetic Perturbations in DIII-D

by
M.R. Wade for the DIII-D
ELM Control Task Force

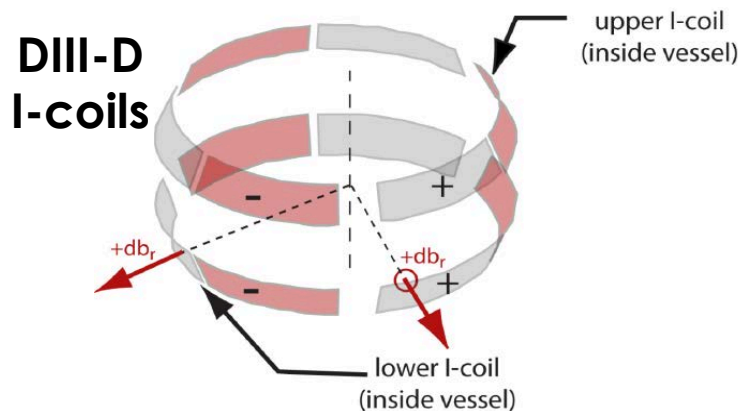
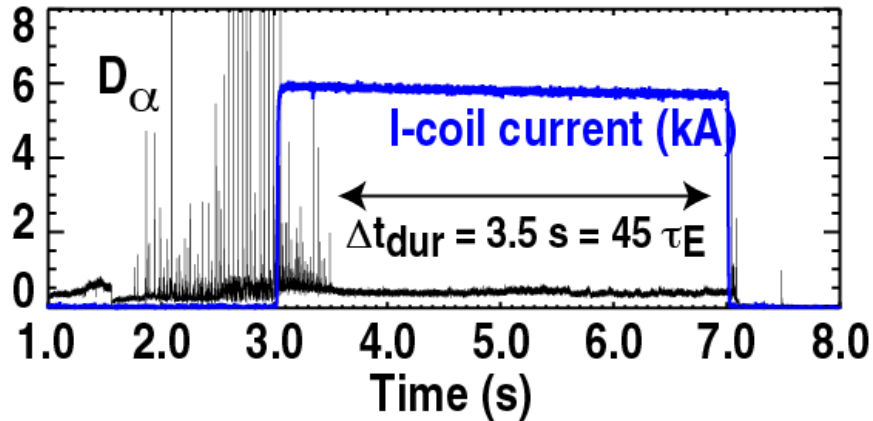
Presented at
2012 IAEA Fusion
Energy Conference
San Diego, California

October 8–13, 2012

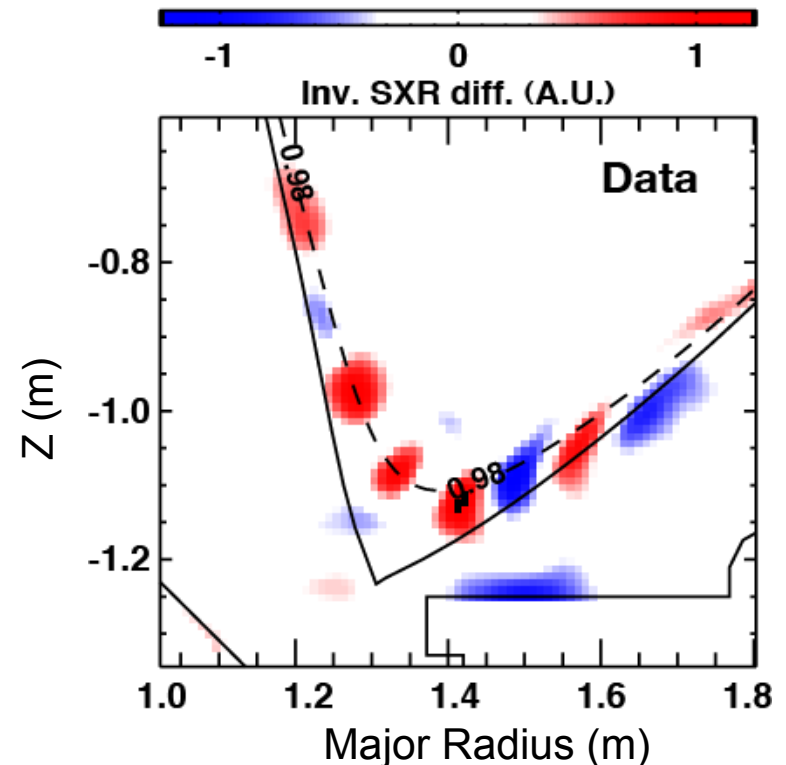


DIII-D Research Has Increased Confidence in Ability to Achieve RMP ELM Suppression on ITER

- ELM suppression operating space expanded to include ITER baseline

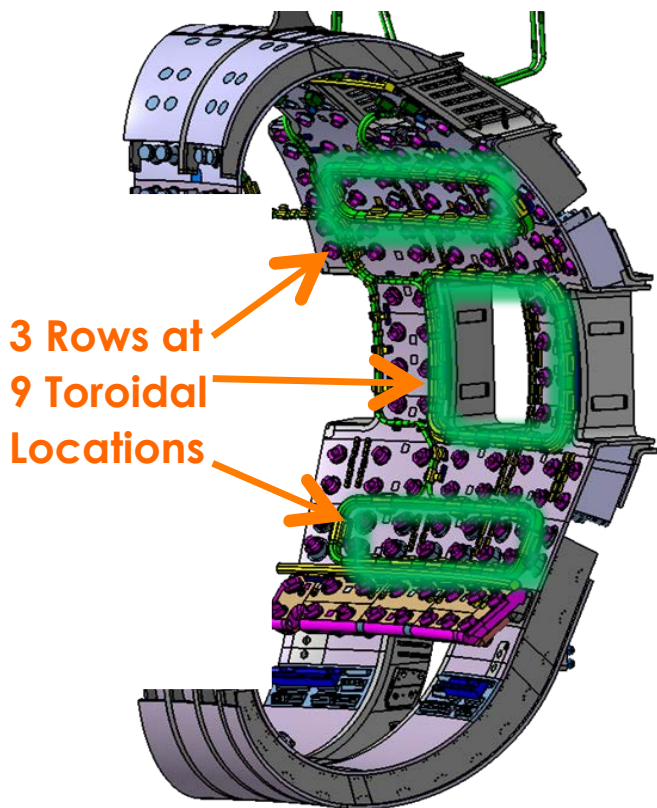


- Significant advances in physics understanding of RMP effects



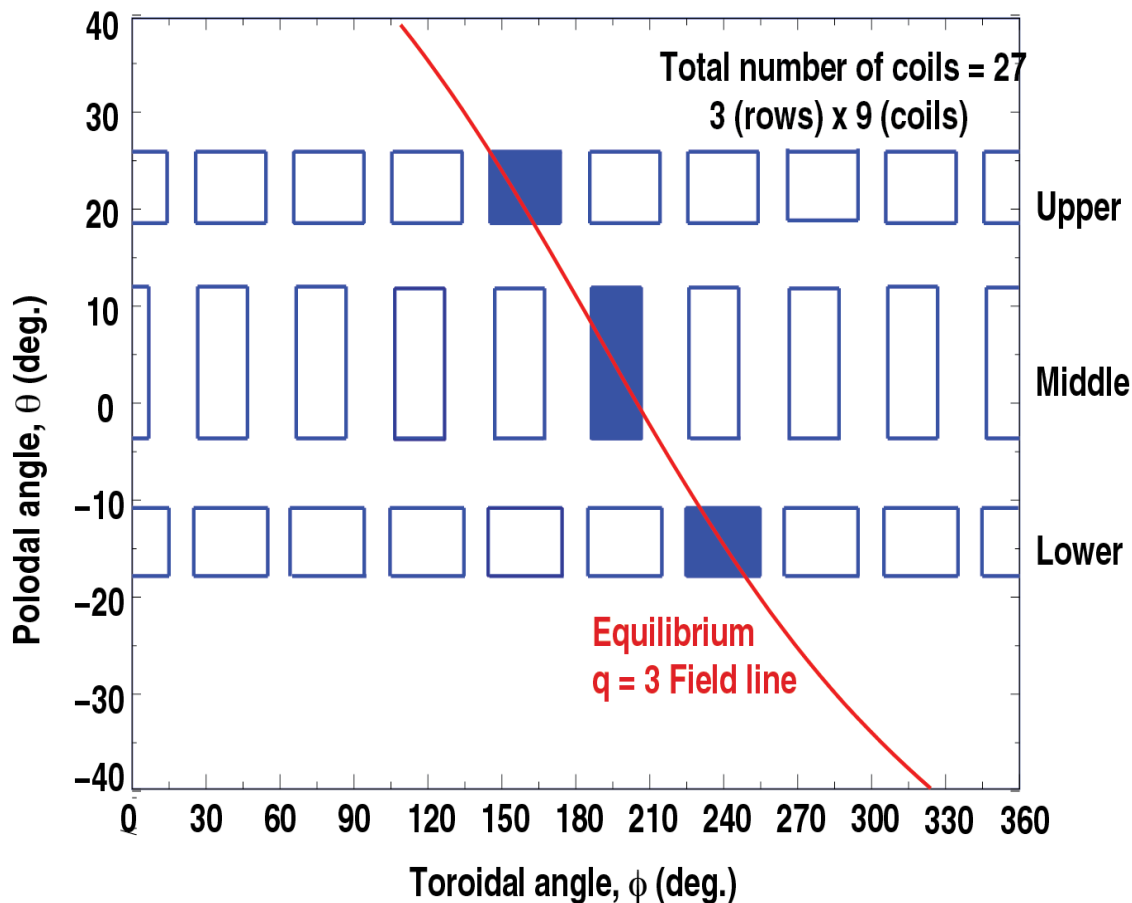
ITER Design Incorporates 3D Coil Set for Producing Magnetic Perturbations Localized in the Edge

ITER ELM Control Coils



Goal: Generate 3D field that is pitch-aligned to the edge equilibrium field

ITER ELM Coil (IEC) θ, ϕ Geometry



ELM Suppression Sustained for Long Duration in ITER Baseline Scenario

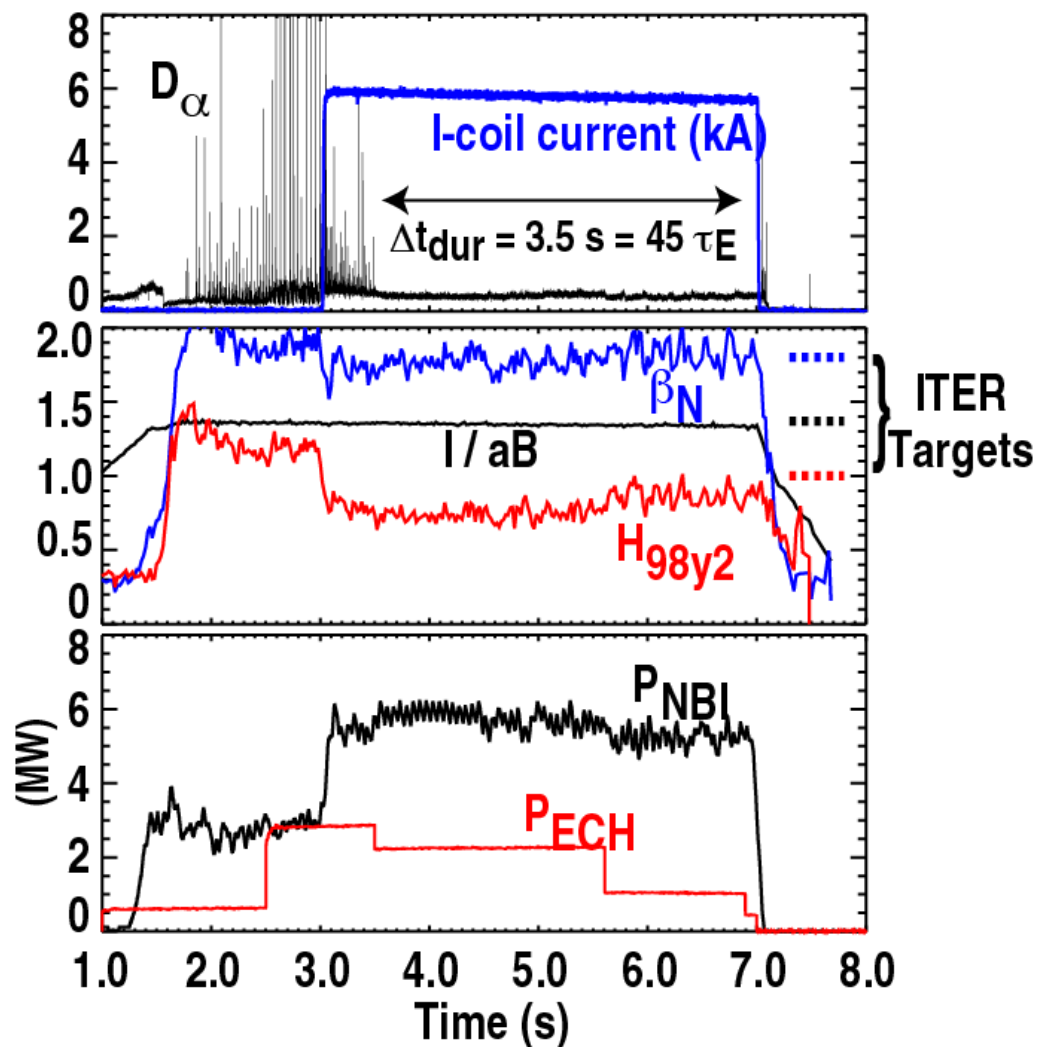
- Sustained for 3.5 s, limited only by technical limits of power supplies
- Approximates ITER baseline specifications closely:



	I/aB	β_N	H ₉₈	v _{*,ped}
DIII-D	1.40	1.8	0.9	0.12
ITER	1.41	1.8	1.0	0.10

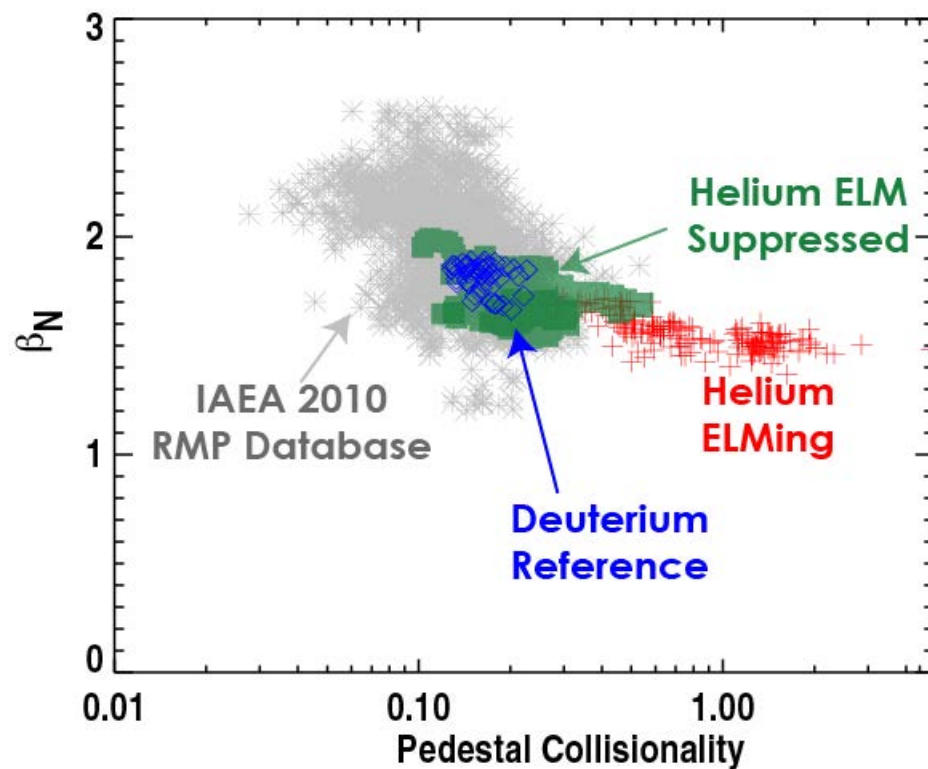
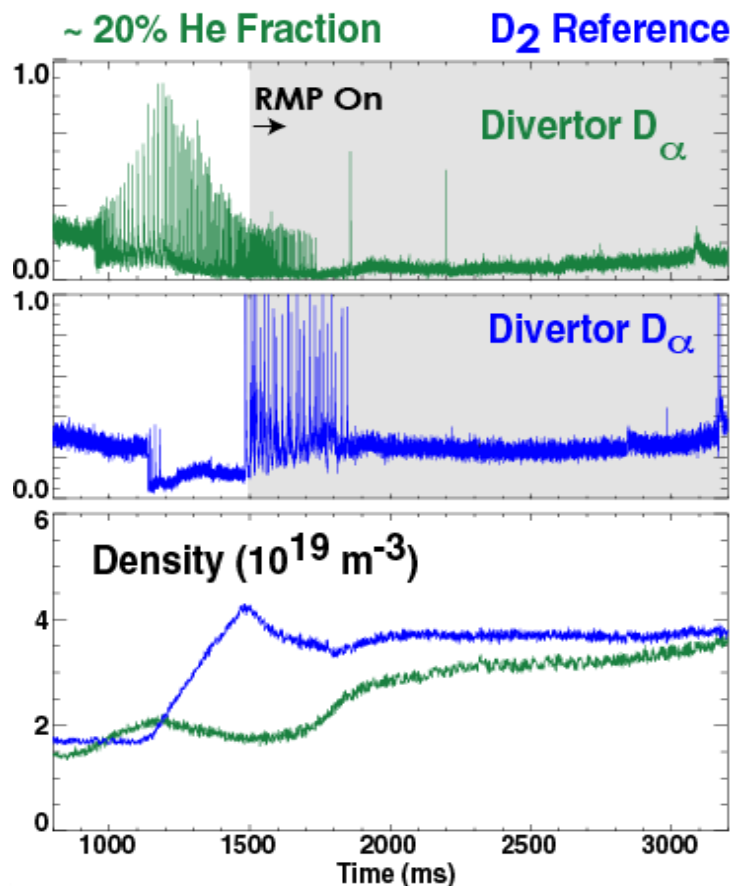
- Achieved with n=3 RMP from single row of I-coils

Proof-of-principle that RMP ELM suppression can be achieved in ITER baseline scenario



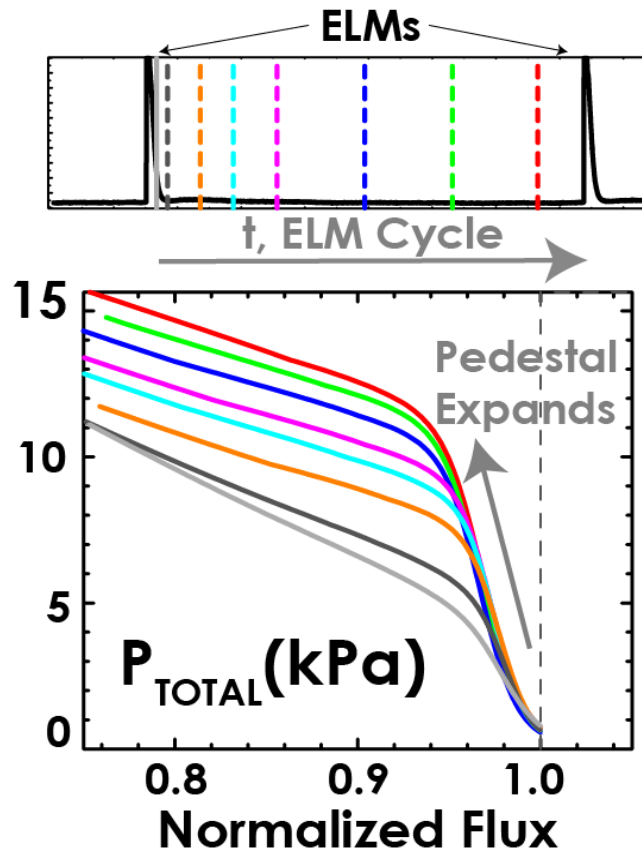
Feasibility of RMP ELM Suppression in ITER Non-Nuclear Phase Demonstrated

- RMP ELM suppression demonstrated in plasmas with up to 25% helium fraction (n_{He}/n_e)
- Transition to ELMs occurs at density and collisionality levels consistent with deuterium database



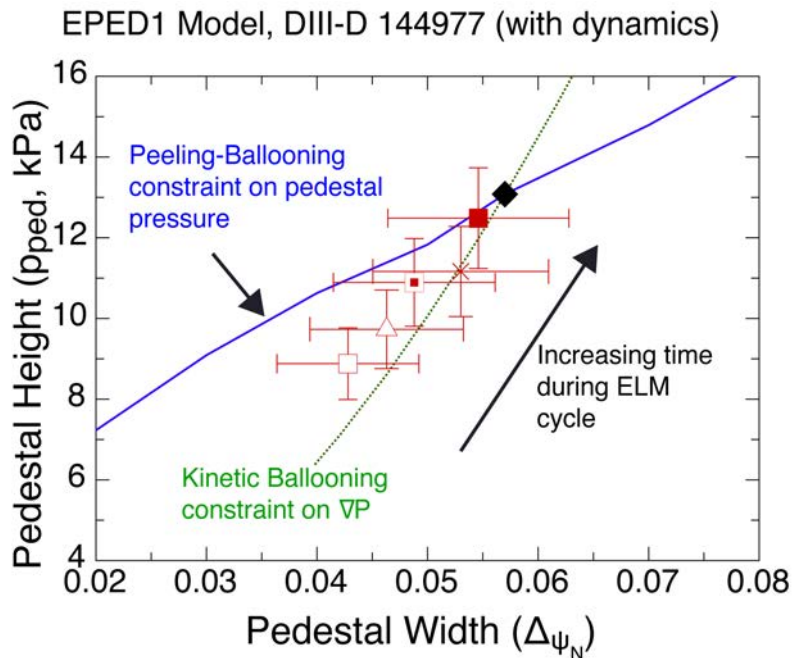
Emerging Model for RMP ELM Suppression

- In non-RMP H-mode, pedestal continues to expand until ELM is encountered



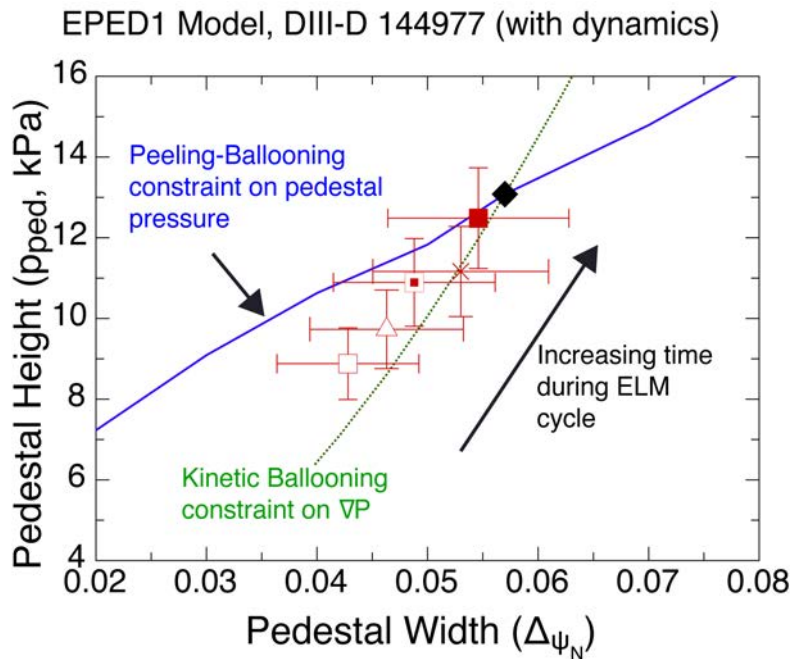
Emerging Model for RMP ELM Suppression

- In non-RMP H-mode, pedestal continues to expand until ELM is encountered
 - Consistent with EPED1 model

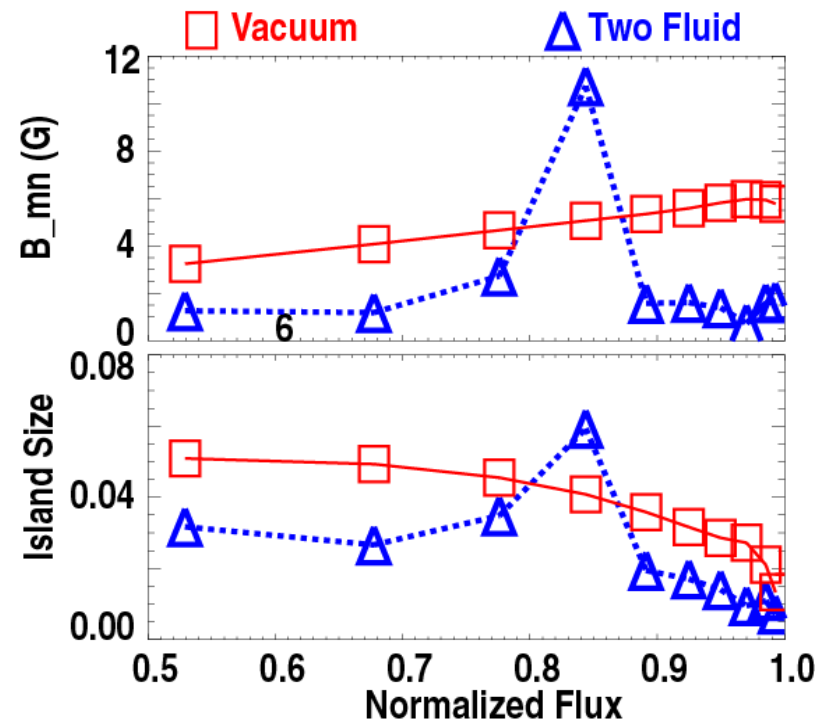


Emerging Model for RMP ELM Suppression

- In non-RMP H-mode, pedestal continues to expand until ELM is encountered
 - Consistent with EPED1 model

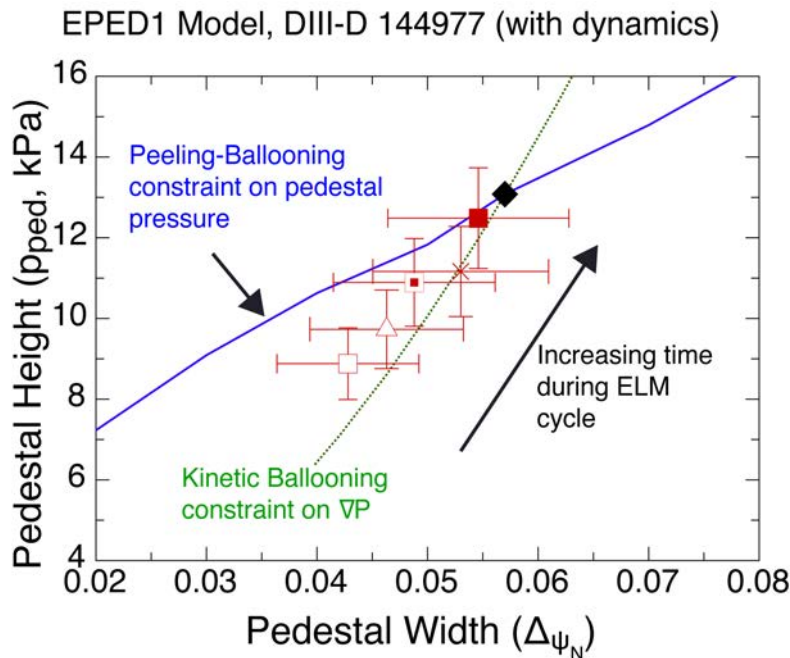


- Model: MHD response at top of pedestal enhances transport and stops pedestal expansion

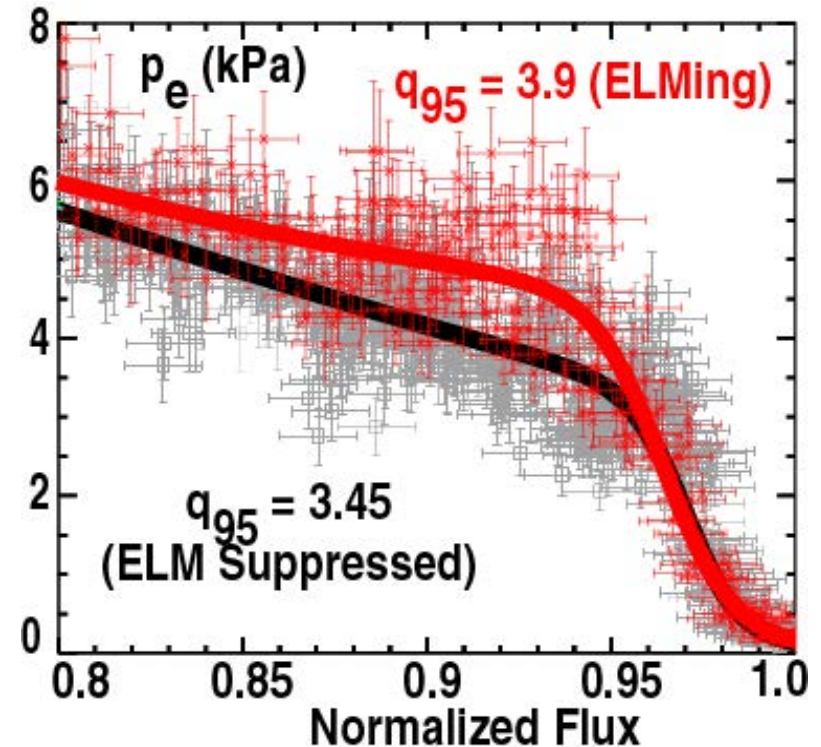


Emerging Model for RMP ELM Suppression

- In non-RMP H-mode, pedestal continues to expand until ELM is encountered
 - Consistent with EPED1 model

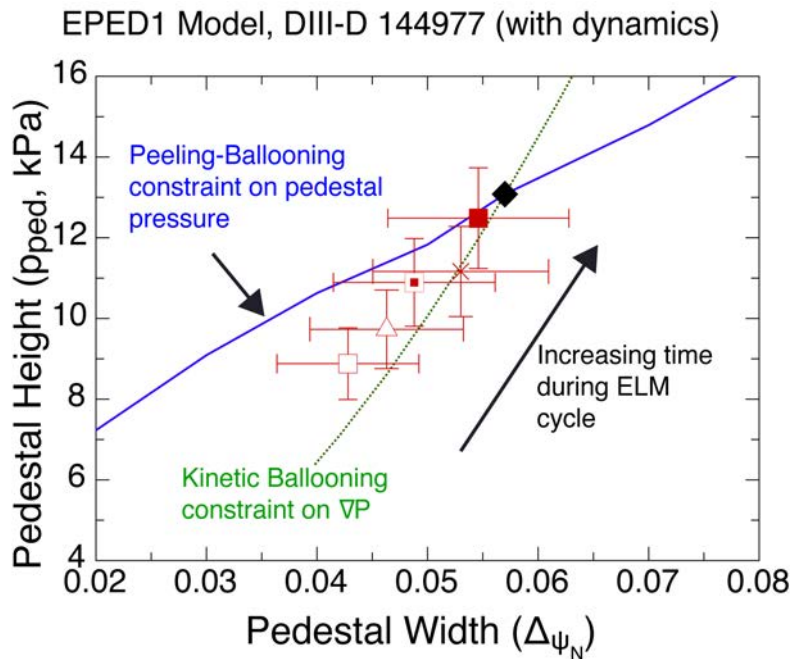


- Model: MHD response at top of pedestal enhances transport and stops pedestal expansion

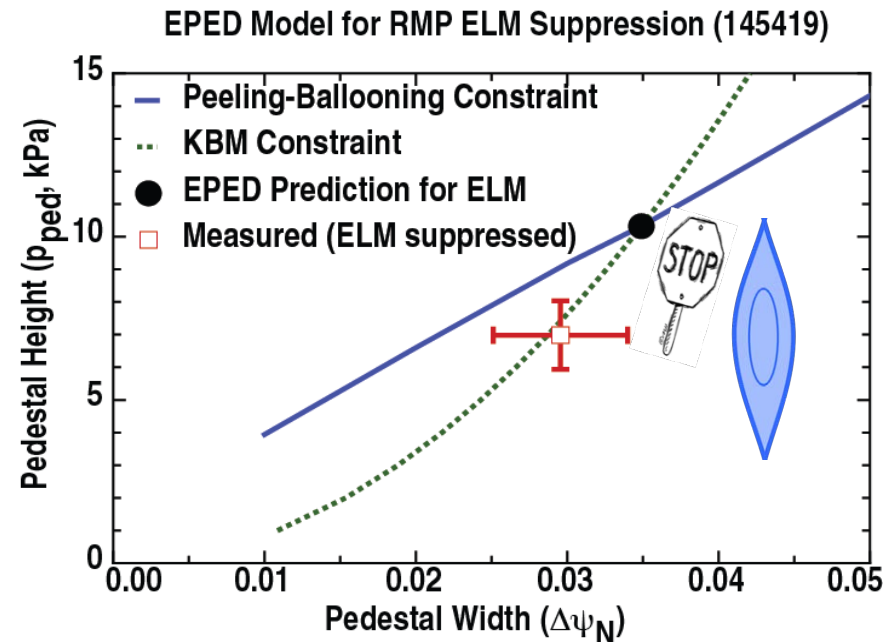


Emerging Model for RMP ELM Suppression

- In non-RMP H-mode, pedestal continues to expand until ELM is encountered
 - Consistent with EPED1 model

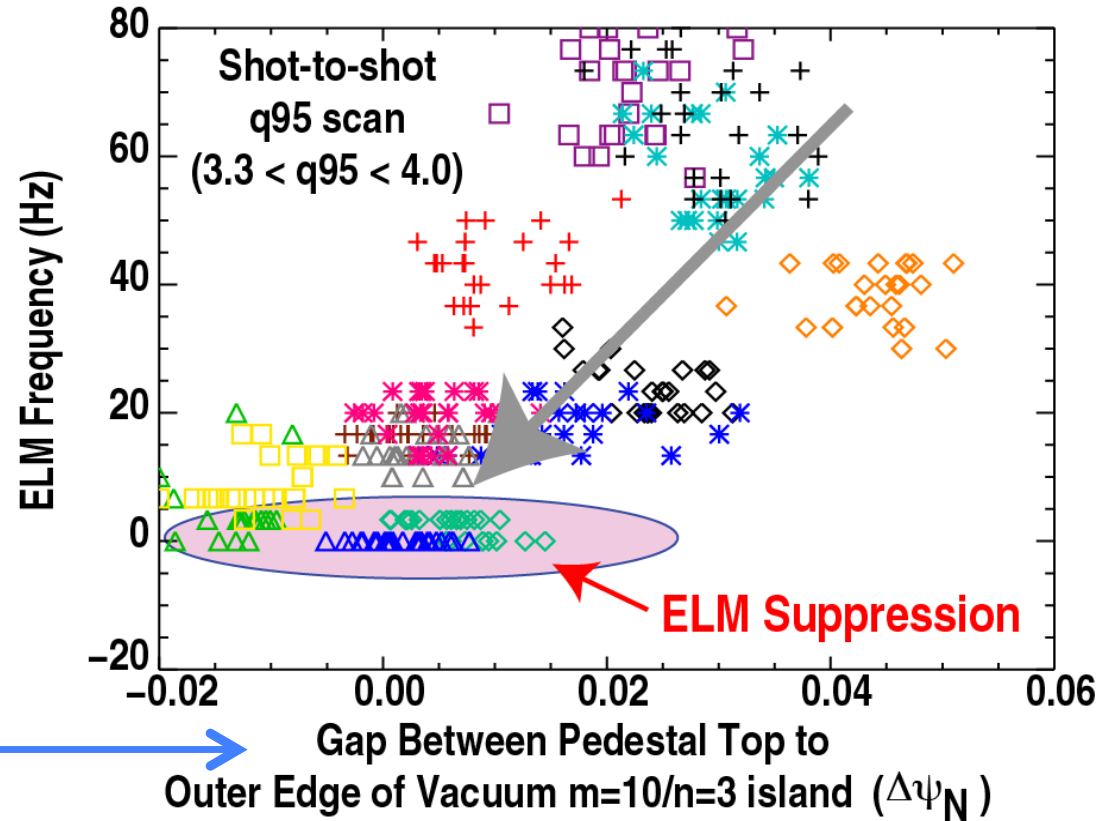
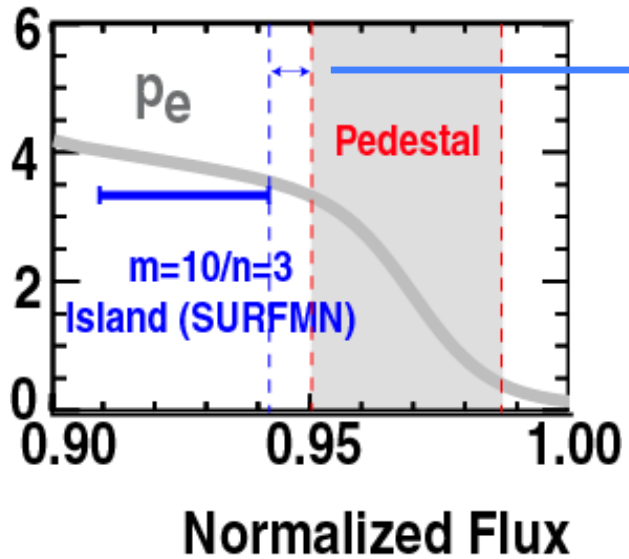


- Model: MHD response at top of pedestal enhances transport and stops pedestal expansion
 - Avoiding ELM instability boundary



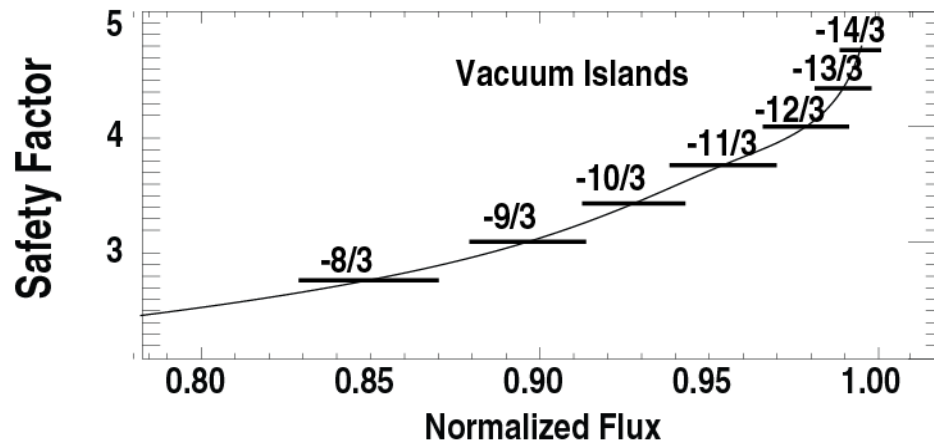
Degree of ELM Mitigation Correlated with Alignment of Pedestal Top and Outer Extent of $m=10/n=3$ Island

- Island location and widths based on SURFMN vacuum field analysis



Two-Fluid Resistive Codes Predict Shielding Currents on Rational Surfaces Modify Plasma Response Significantly

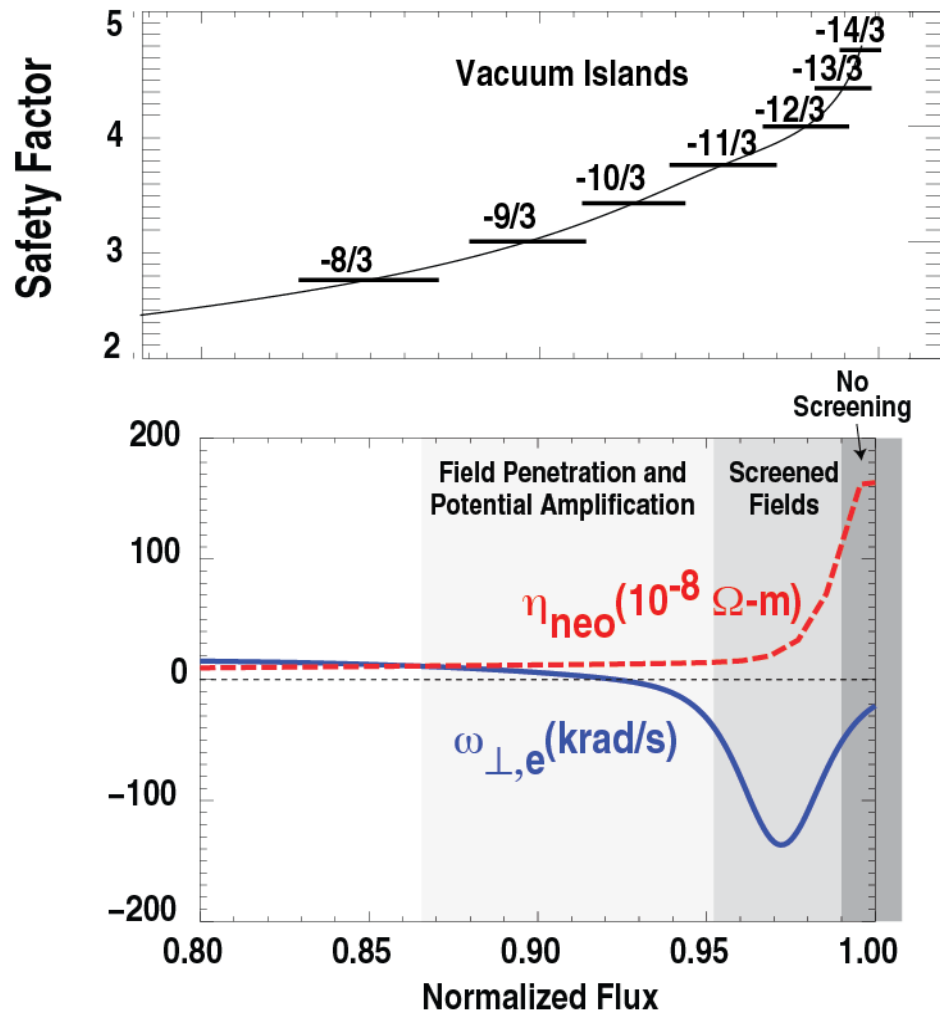
- In vacuum model, large islands generated in edge region
- Applied field shielded by image currents on rational surface if:
 - Resistivity is small (true everywhere but edge)
 - Sufficient plasma rotation



Two-Fluid Resistive Codes Predict Shielding Currents on Rational Surfaces Modify Plasma Response Significantly

- In vacuum model, large islands generated in edge region
- Applied field shielded by image currents on rational surface if:
 - Resistivity is small (true everywhere but edge)
 - Sufficient plasma rotation
- Fields can “penetrate” at low perpendicular electron frequency

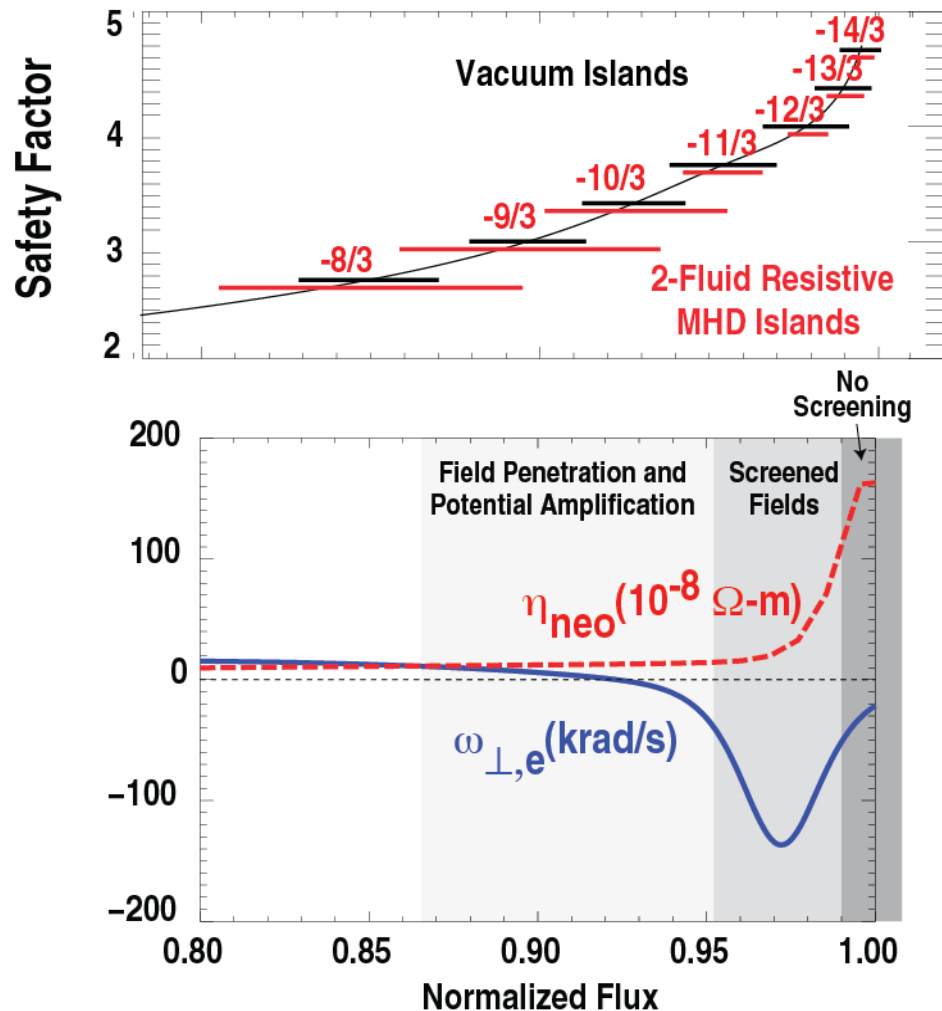
$$\omega_{\perp,e} = \omega_{ExB} + \omega_{e,dia}$$



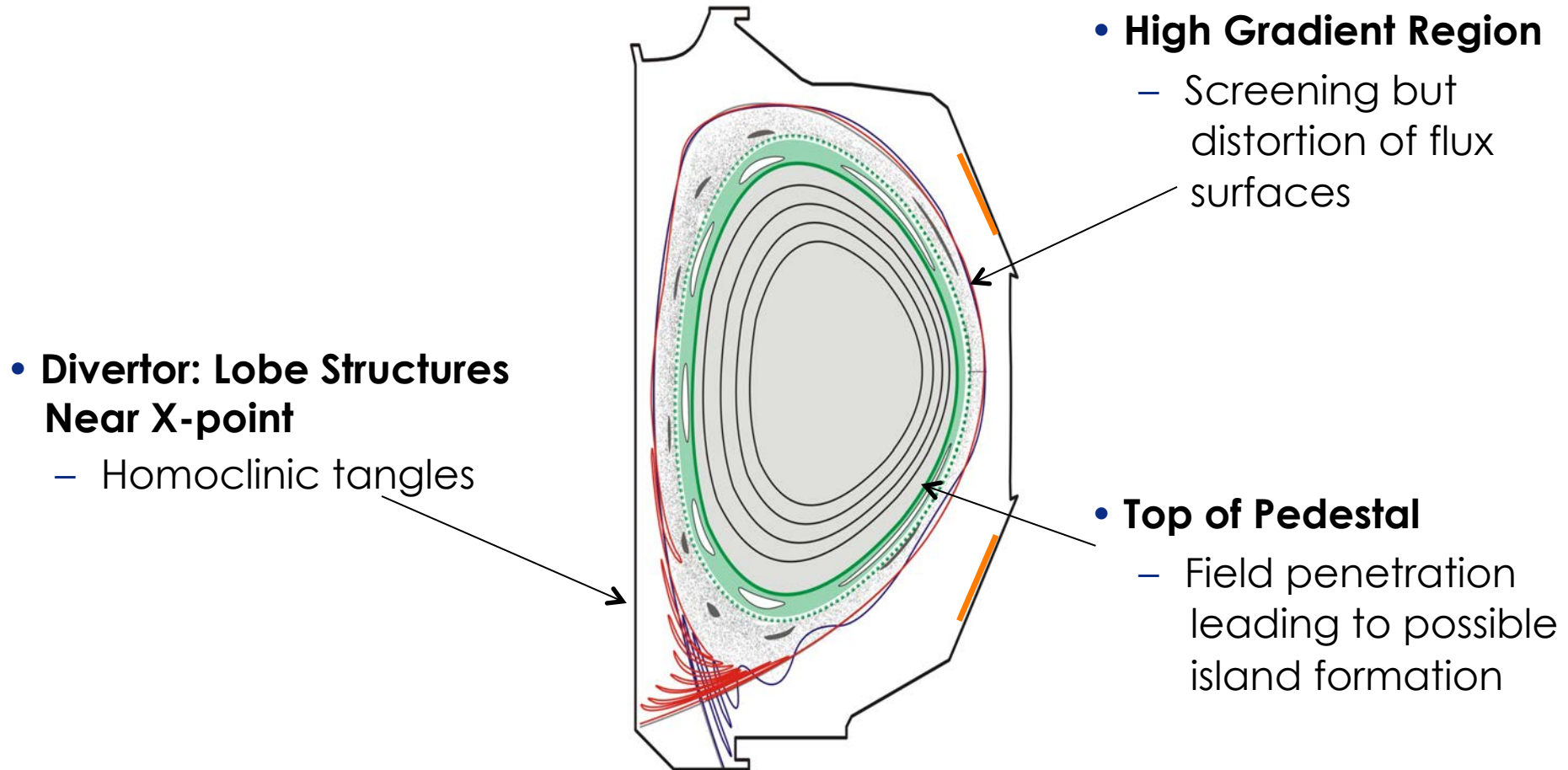
Two-Fluid Resistive Codes Predict Shielding Currents on Rational Surfaces Modify Plasma Response Significantly

- In vacuum model, large islands generated in edge region
- Applied field shielded by image currents on rational surface if:
 - Resistivity is small (true everywhere but edge)
 - Sufficient plasma rotation
- Fields can “penetrate” at low perpendicular electron frequency

$$\omega_{\perp,e} = \omega_{ExB} + \omega_{e,dia}$$
- **2-Fluid model predicts larger islands at top of pedestal, smaller in barrier**



Three Distinct Regions of Plasma Response are Predicted by Two-Fluid Resistive Code M3D-C1

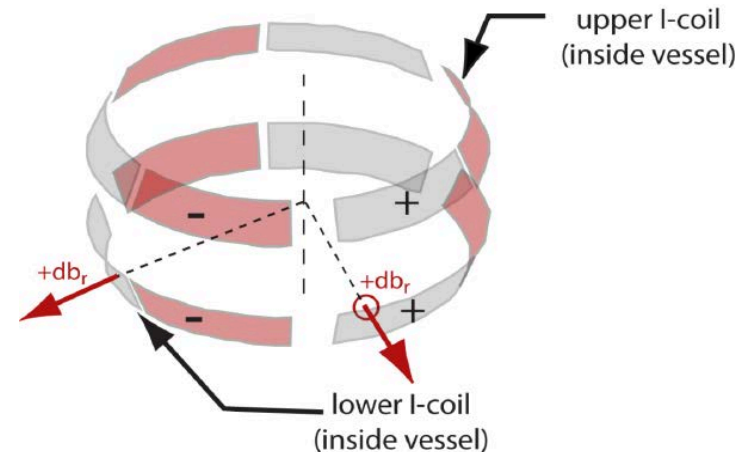
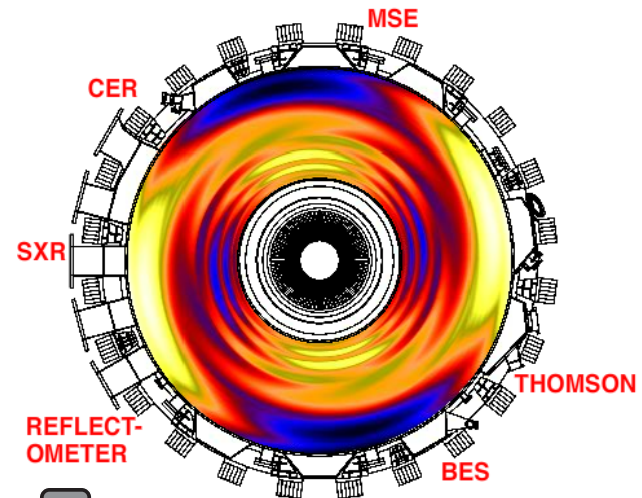


Toroidal Phase Variations of Applied RMP Used to Rotate Perturbations Across Toroidally Fixed Diagnostics

- Diagnostic locations are fixed
 - Can only sample local perturbation
- However, RMP can be rotated with respect to diagnostics to measure toroidal variation of perturbation
- DIII-D I-coil set has 6 coils per row allowing
 - $n=2$ Full toroidal rotation
 - $n=3$ Only two toroidal phases separated by 60° toroidally

Top View

$n = 2 B_r$ at midplane

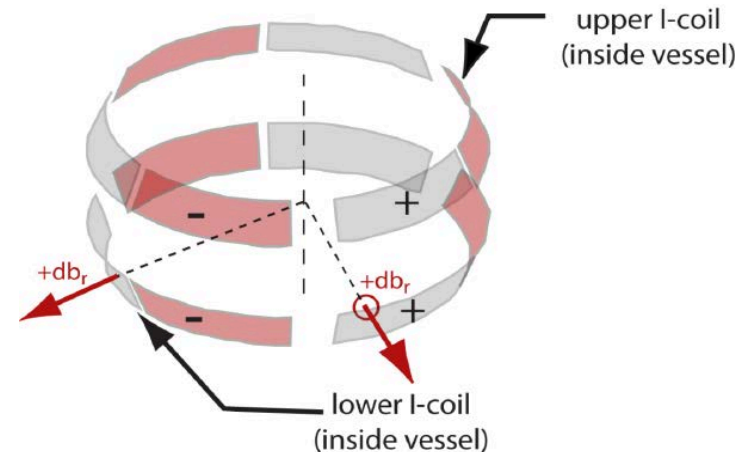
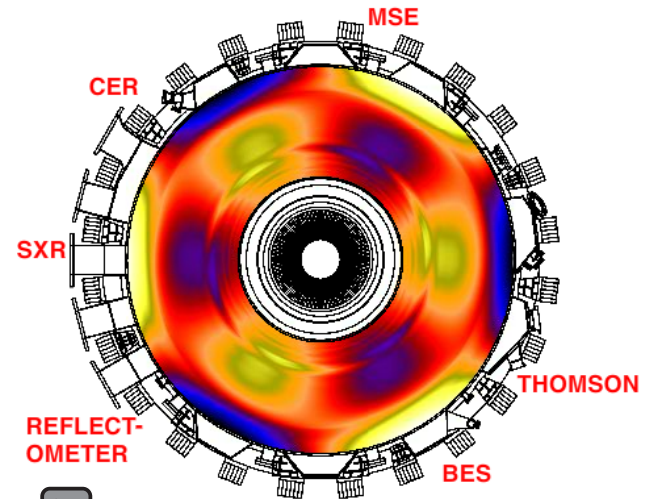


Toroidal Phase Variations of Applied RMP Used to Rotate Perturbations Across Toroidally Fixed Diagnostics

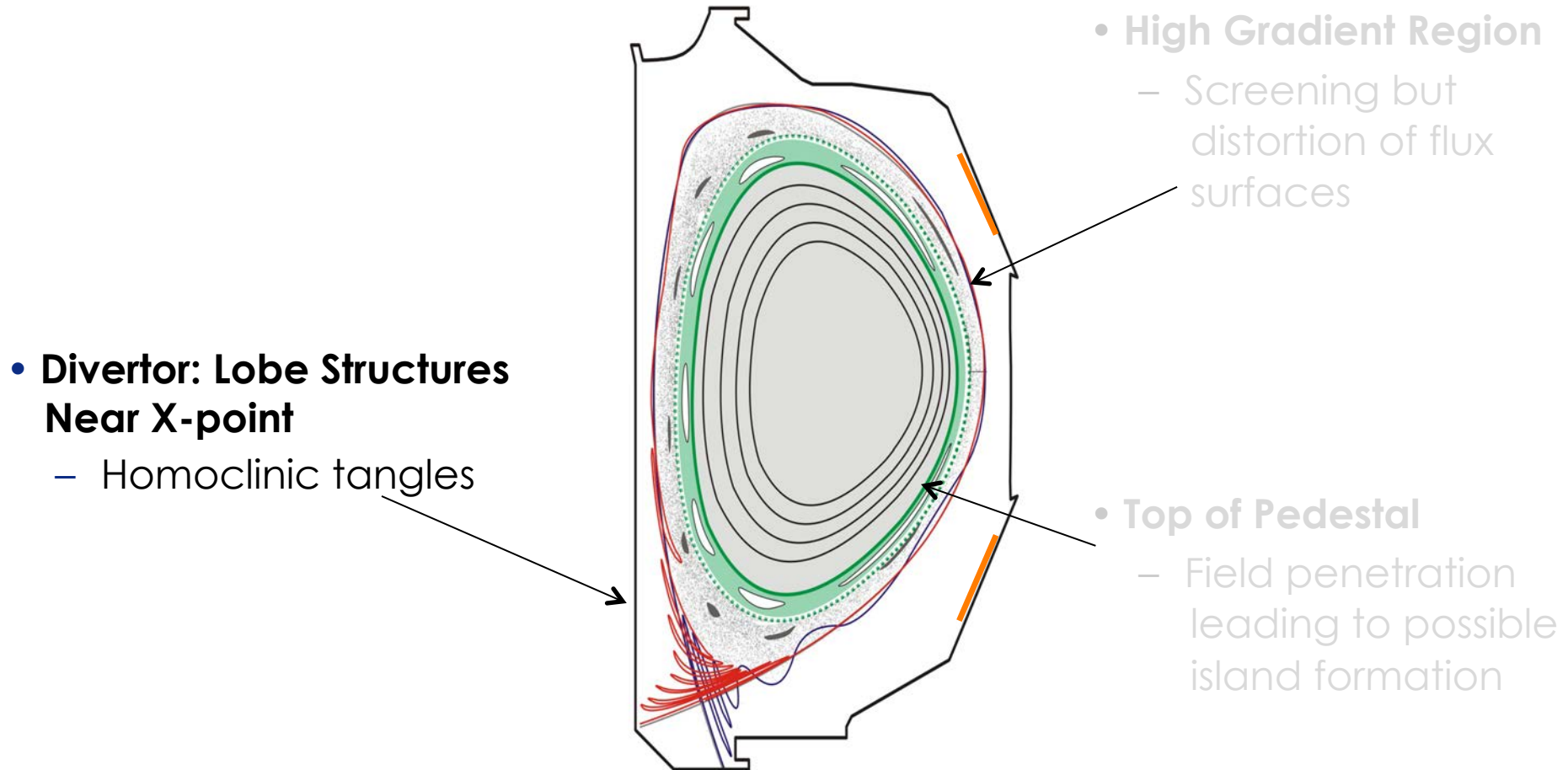
- Diagnostic locations are fixed
 - Can only sample local perturbation
- However, RMP can be rotated with respect to diagnostics to measure toroidal variation of perturbation
- DIII-D I-coil set has 6 coils per row allowing
 - $n=2$ Full toroidal rotation
 - $n=3$ Only two toroidal phases separated by 60° toroidally

Top View

$n = 3 B_r$ at midplane

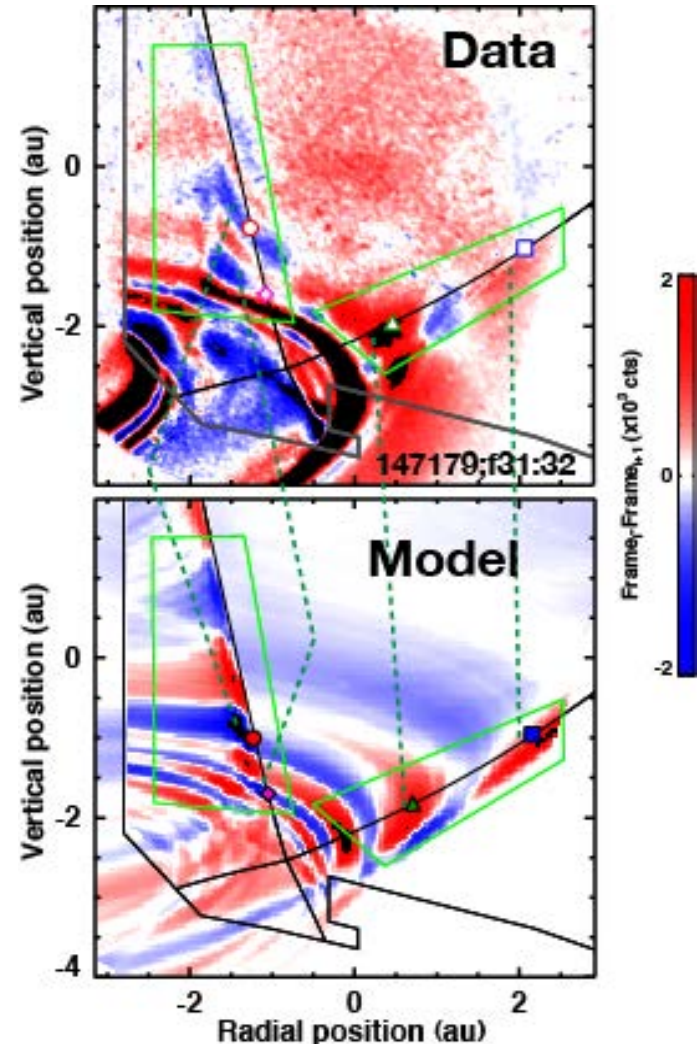


Three Distinct Regions of Plasma Response are Predicted by Two-Fluid Resistive Code M3D-C1



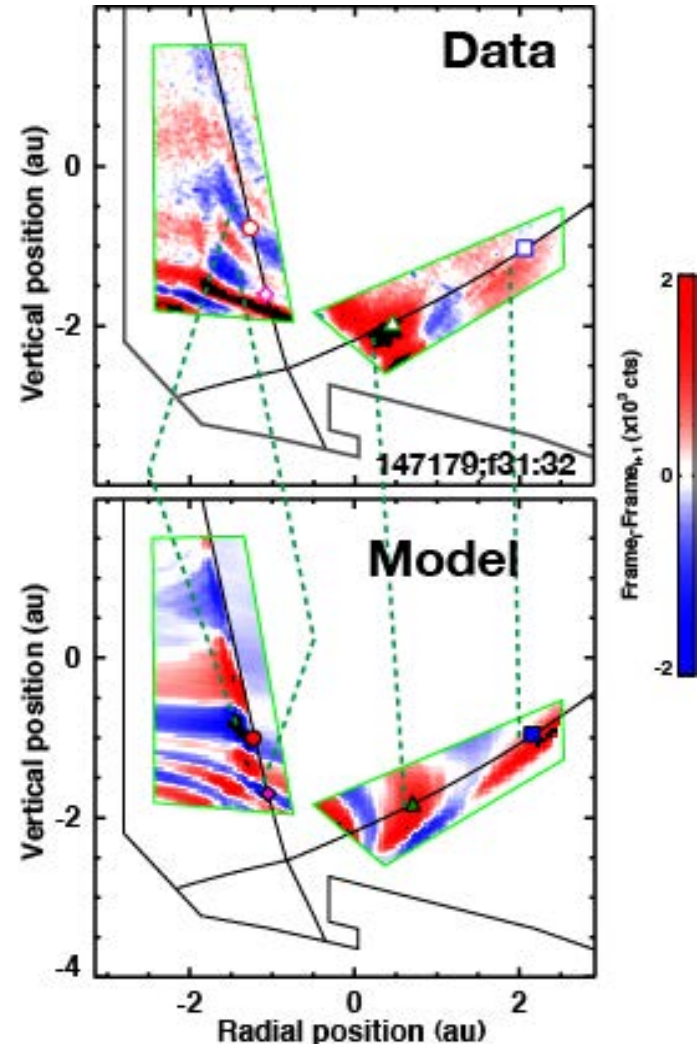
Vacuum Model Qualitatively Describes Observation of Homoclinic Tangles in Divertor

- Strike-point splitting with q_{95} variation predicted by vacuum model
- Extreme soft X-ray imaging detects lobe structures at X-point
 - Homoclinic tangles
- Large floating potential detected on divertor probes when predicted lobe location coincident with probe

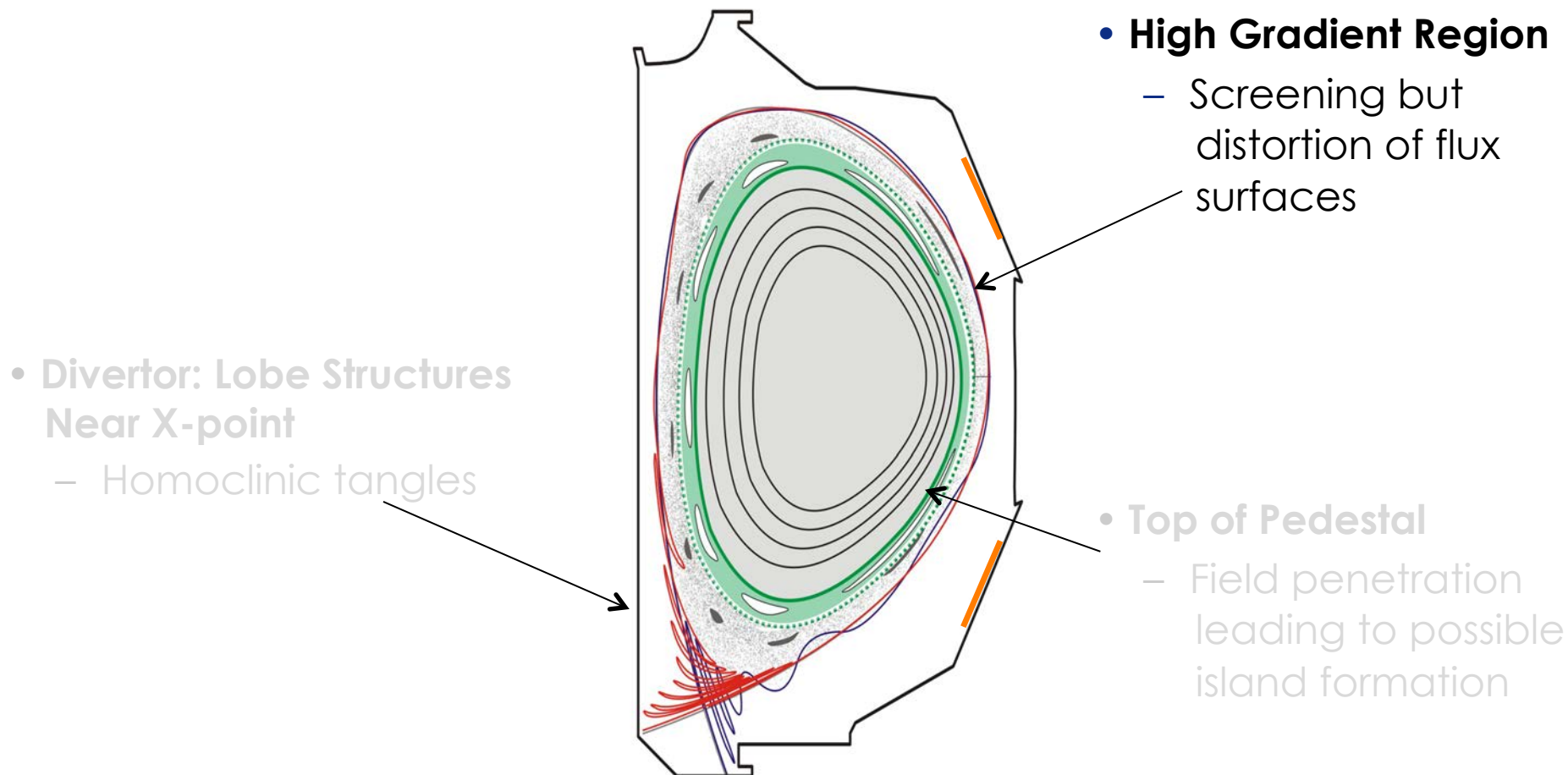


Vacuum Model Qualitatively Describes Observation of Homoclinic Tangles in Divertor

- Strike-point splitting with q_{95} variation predicted by vacuum model
- Extreme soft X-ray imaging detects lobe structures at X-point
 - Homoclinic tangles
- Large floating potential detected on divertor probes when predicted lobe location coincident with probe

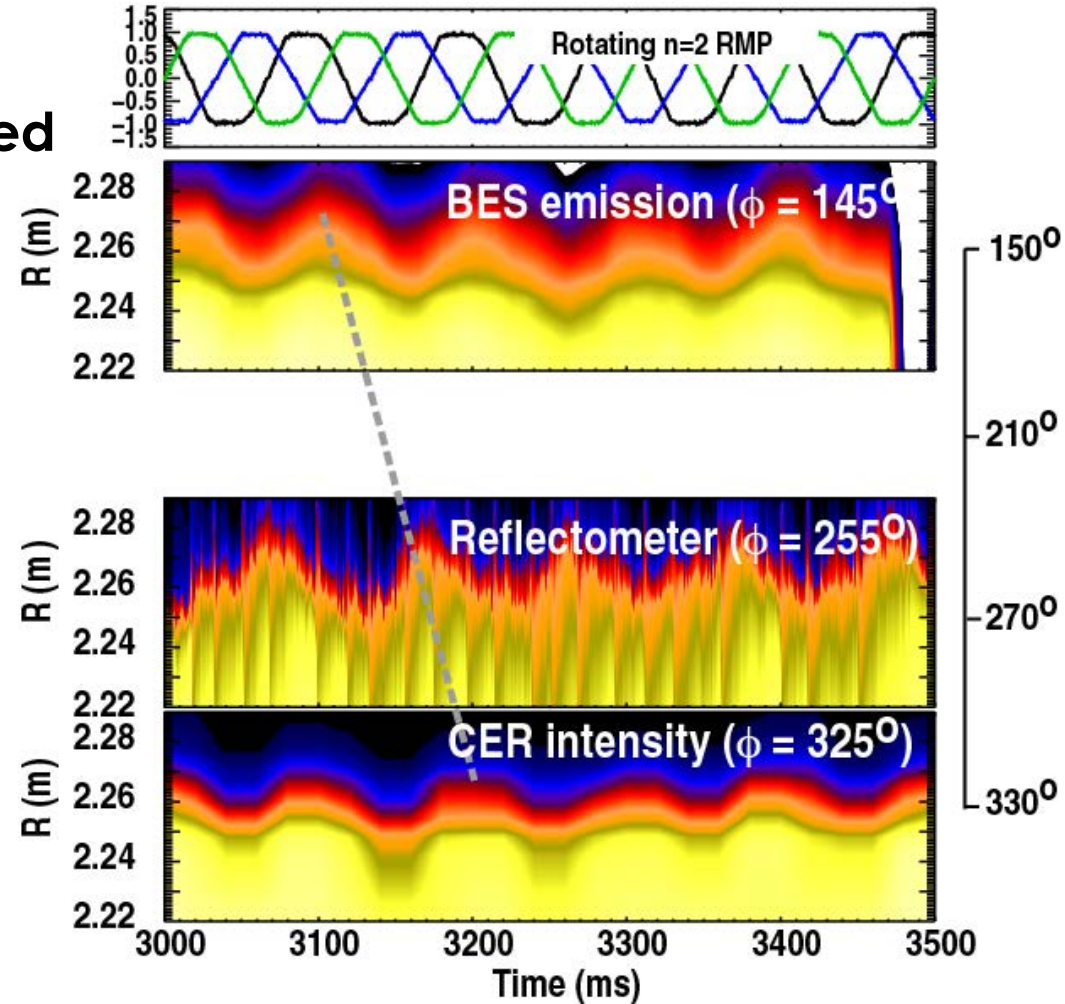


Three Distinct Regions of Plasma Response are Predicted by Two-Fluid Resistive Code M3D-C1



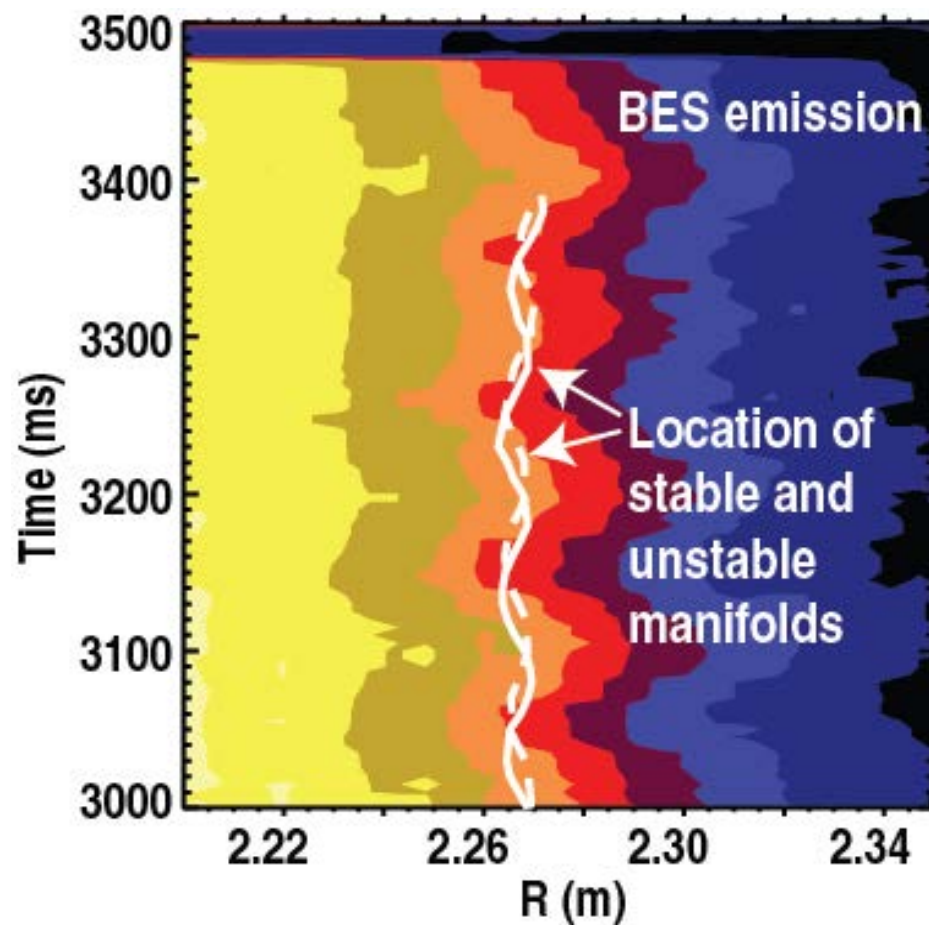
Rotating n=2 RMP Produces Synchronous Modulation of Edge Profiles

- Significant displacements (~2–3 cm) observed at midplane as n=2 RMP is rotated
- Toroidal variation of measurements confirms n=2 perturbation structure



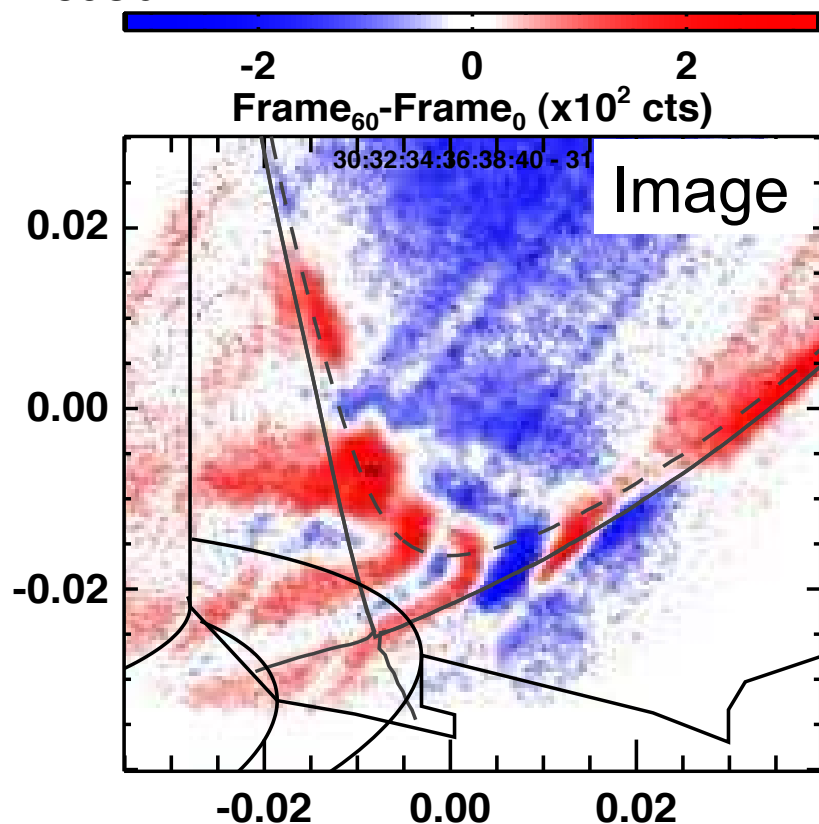
Displacement at Midplane Associated with $n=2$ RMP Much Larger than Vacuum Prediction

- Significant displacements ($\sim 2\text{--}3$ cm) observed at midplane as $n=2$ RMP is rotated
- Toroidal variation of measurements confirms $n=2$ perturbation structure
- Size of displacement is factor of 4–5x larger than vacuum prediction
 - Suggests importance of MHD response to applied field

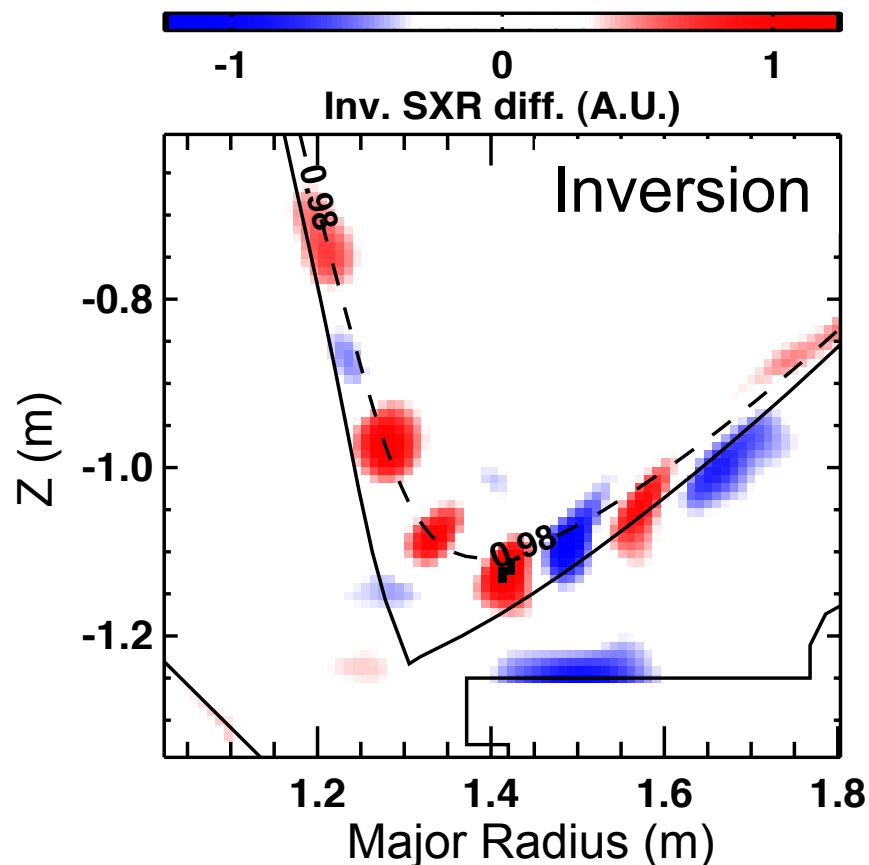


Higher Energy Filter on Soft X-Ray Imaging System Enables Measurements of Internal Helical Structures

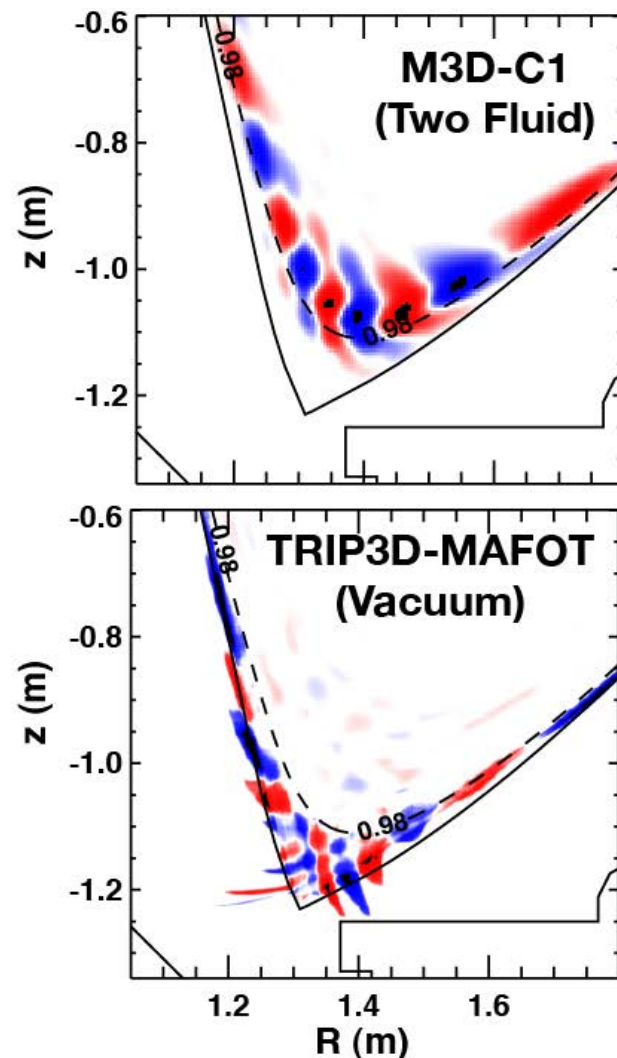
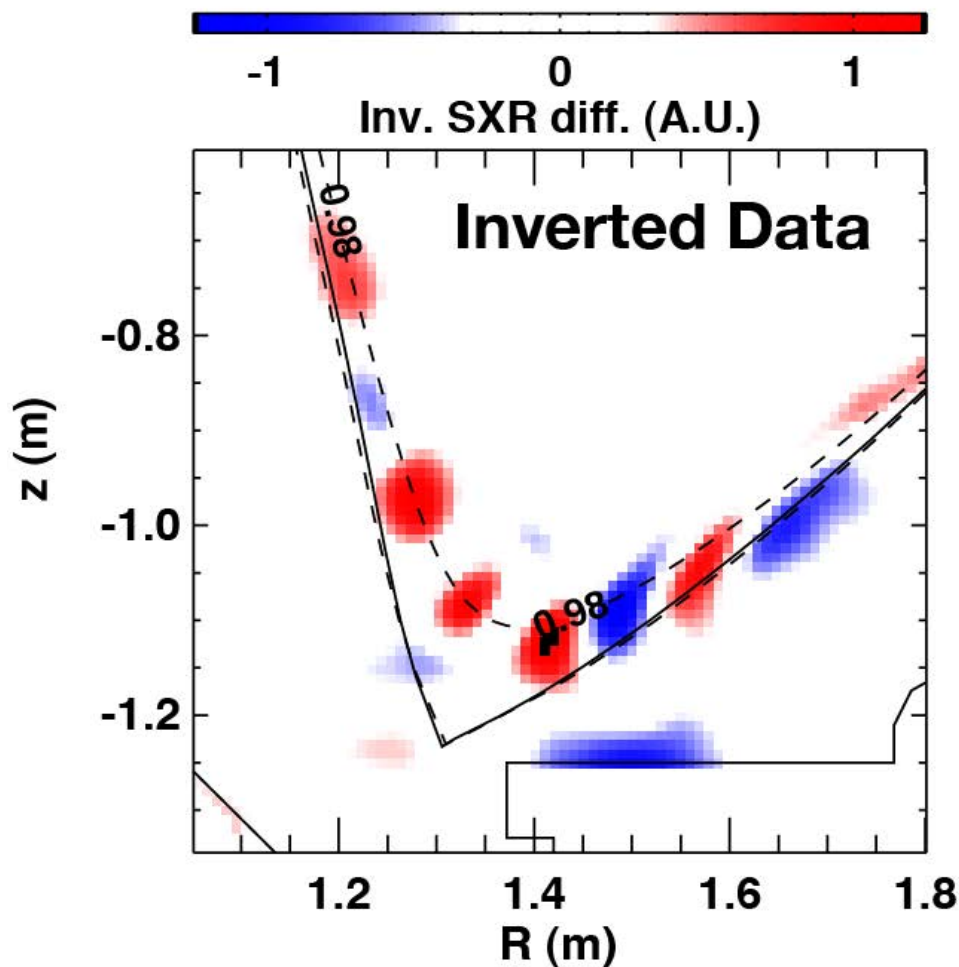
- To accentuate confined plasma emission, high energy (~ 600 eV) filter used



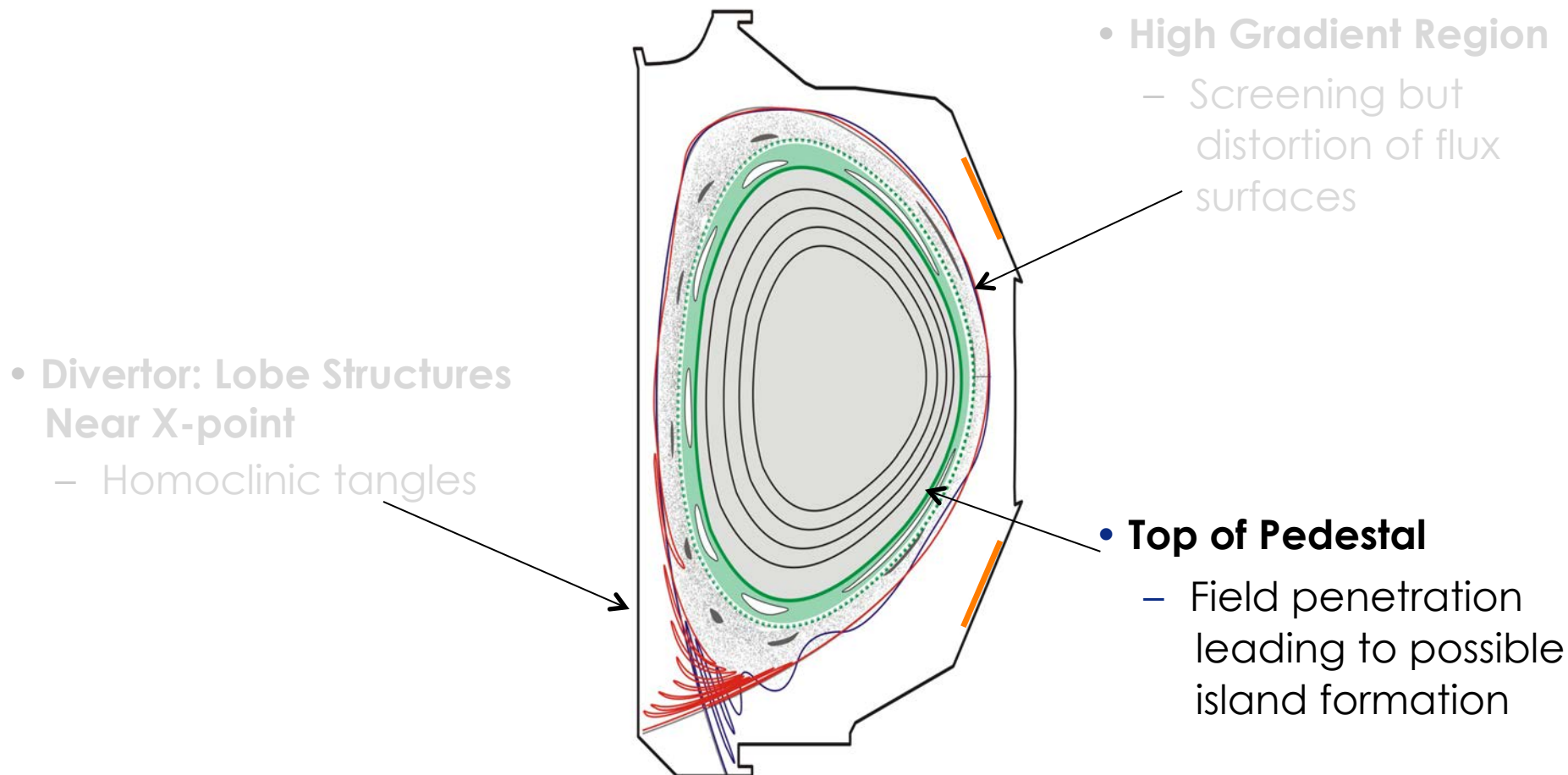
- Tomographic reconstruction reveals internal structures



Comparison Shows Better Agreement with Two-Fluid Resistive MHD Predictions Compared to Vacuum Predictions

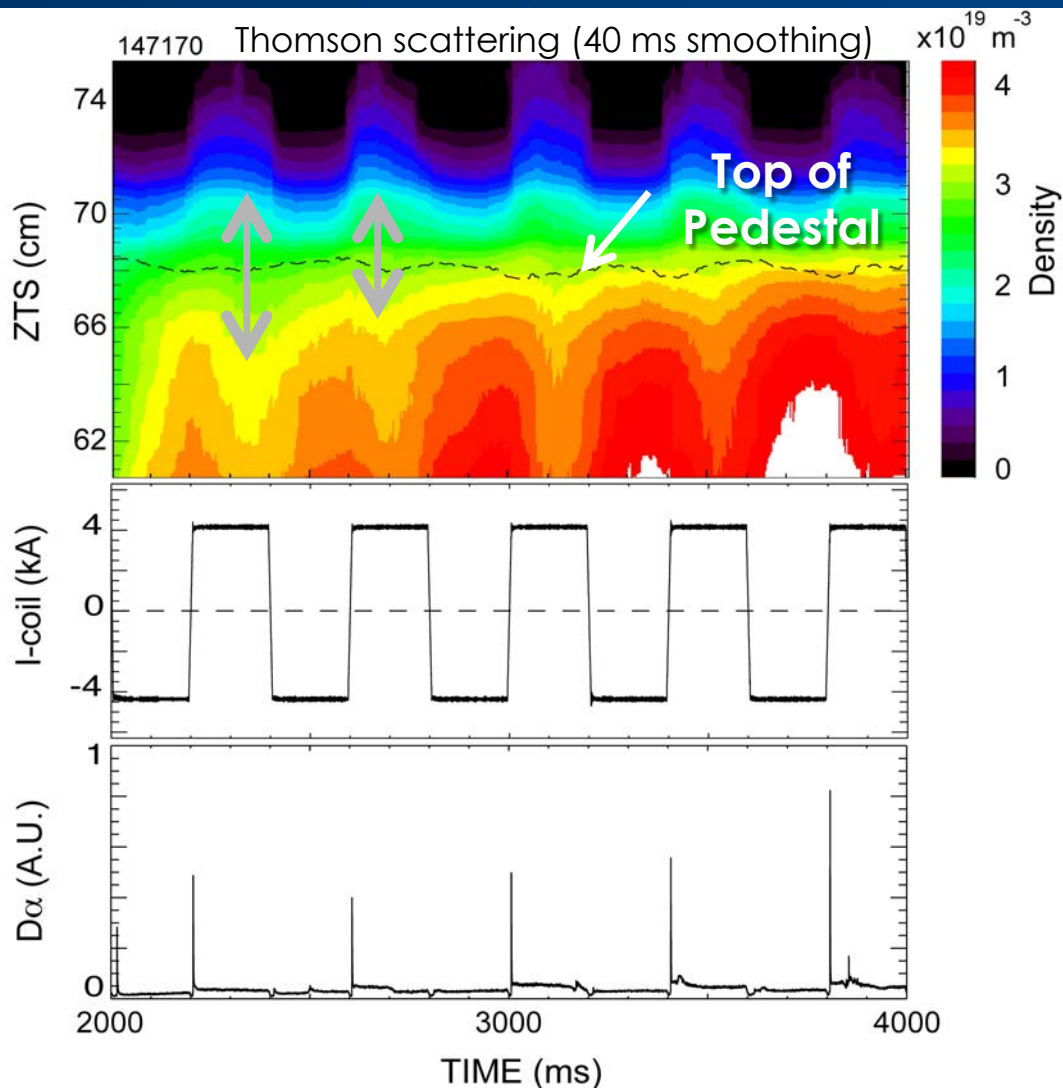


Three Distinct Regions of Plasma Response are Predicted by Two-Fluid Resistive Code M3D-C1



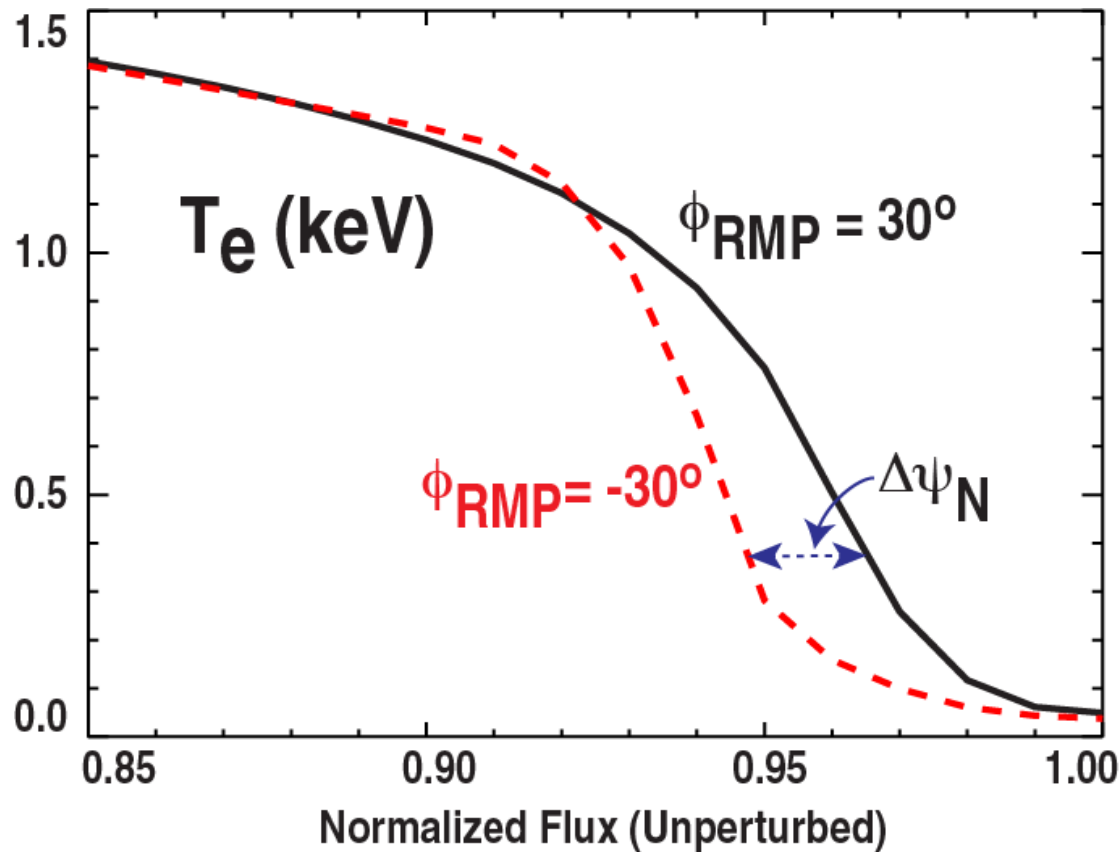
Edge Displacements Accompanied by Island-Like Signature at Top of Pedestal

- Toroidal phase of $n=3$ RMP switched by 60° every 200 ms
- Observe correlated displacement at very edge similar to $n=2$ case
- However, response toward top of pedestal shows phase inversion
 - What causes this??



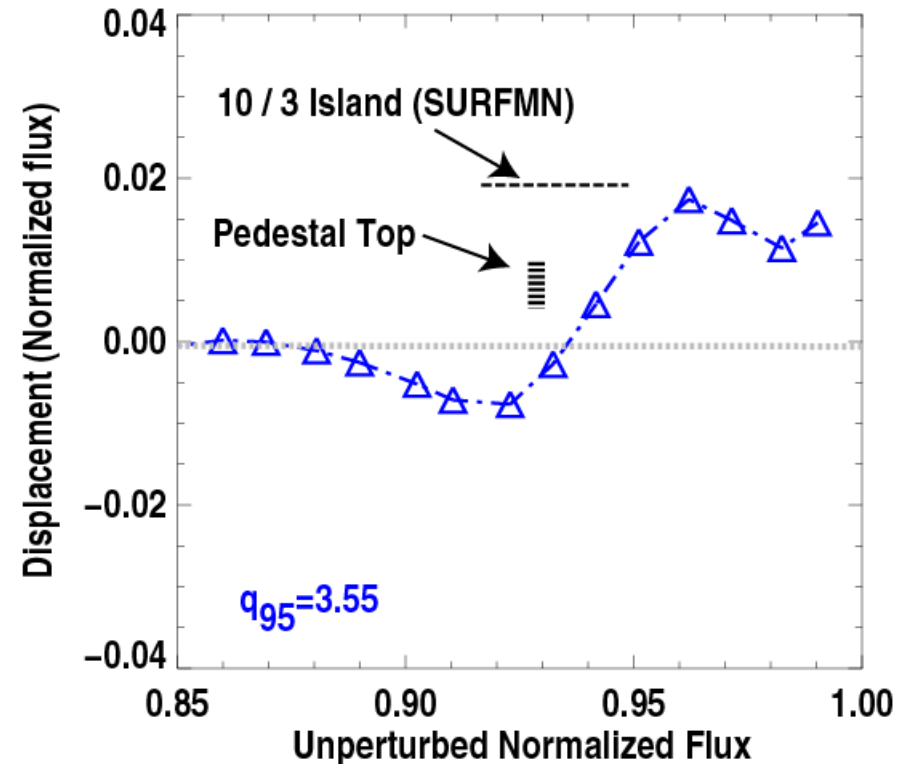
Technique for Estimating Flux Surface Displacement Due to Toroidal Phase Shifts

- Displacement computed assuming change in T_e profile due entirely to flux surface displacement



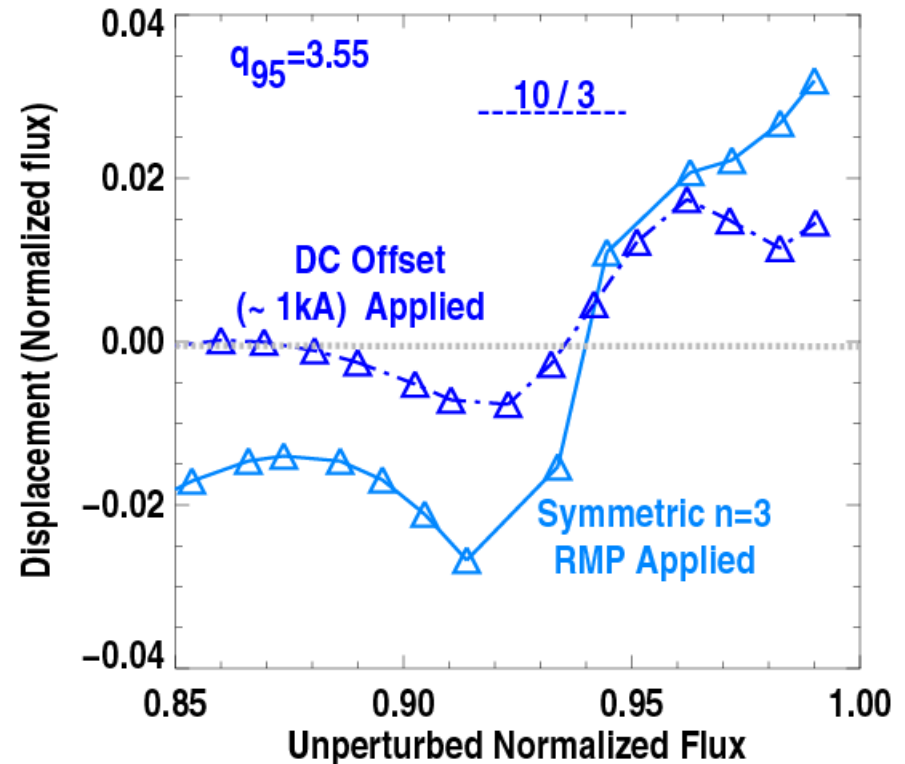
Inferred Displacement Shows Evidence of Island-Like Signature Near Top of Pedestal

- **Significant displacement observed at edge**
 - Similar to $n=2$ observations
- **Phase inversion layer near pedestal top**
- **Island-like signature apparent just inside pedestal top**
 - Coincident with computed location of $m=10/n=3$ island
- **Required compensation of $n=3$ error field to avoid synchronous $n=0$ T_e modulations**



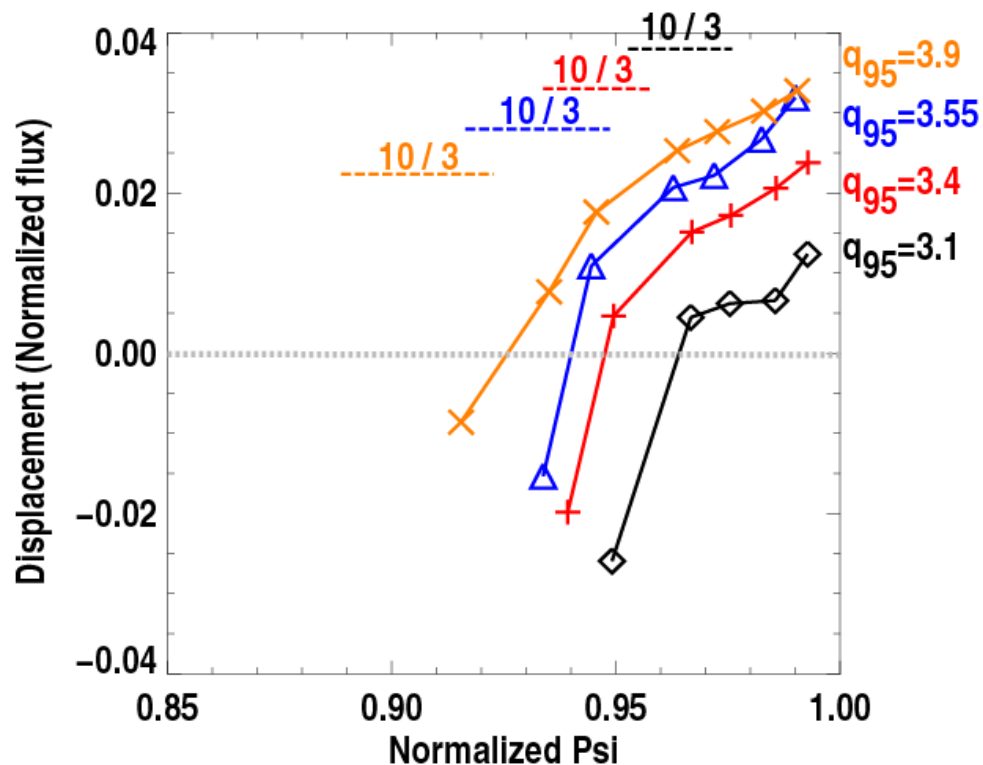
Error Field Interaction Does Not Appear to Strongly Affect Edge Displacement Analysis ($\psi_N > 0.925$)

- Inferred core displacement significantly affected by interaction with n=3 error field
 - Due to n=0 changes in global confinement
- However, edge displacement and phase inversion location does not change appreciably



Edge Displacement Increases with q_{95} and Location of Phase Inversion Layer Track $m=10/n=3$ Island Position

- **Systematic increase in inferred displacement with q_{95}**
 - Also observed with $n=2$ RMP
- **Phase inversion location moves inward as q_{95} increases**
- **Tracks $m=10/n=3$ island position computed by SURFMN**



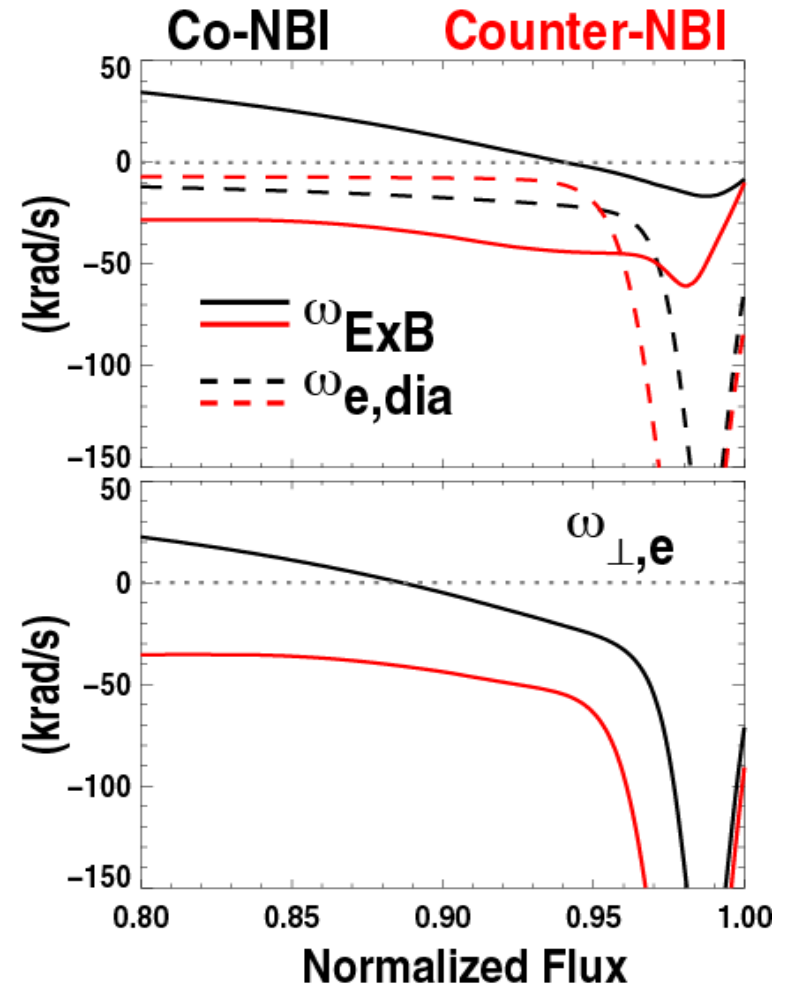
Evidence for island-driven transport??

Counter-NBI Provides Compelling Test of Importance of $\omega_{\perp,e}$ at Top of Pedestal in ELM Suppression

- By switching sign of toroidal rotation, $\omega_{\perp,e} = 0$ crossing at top of pedestal is eliminated

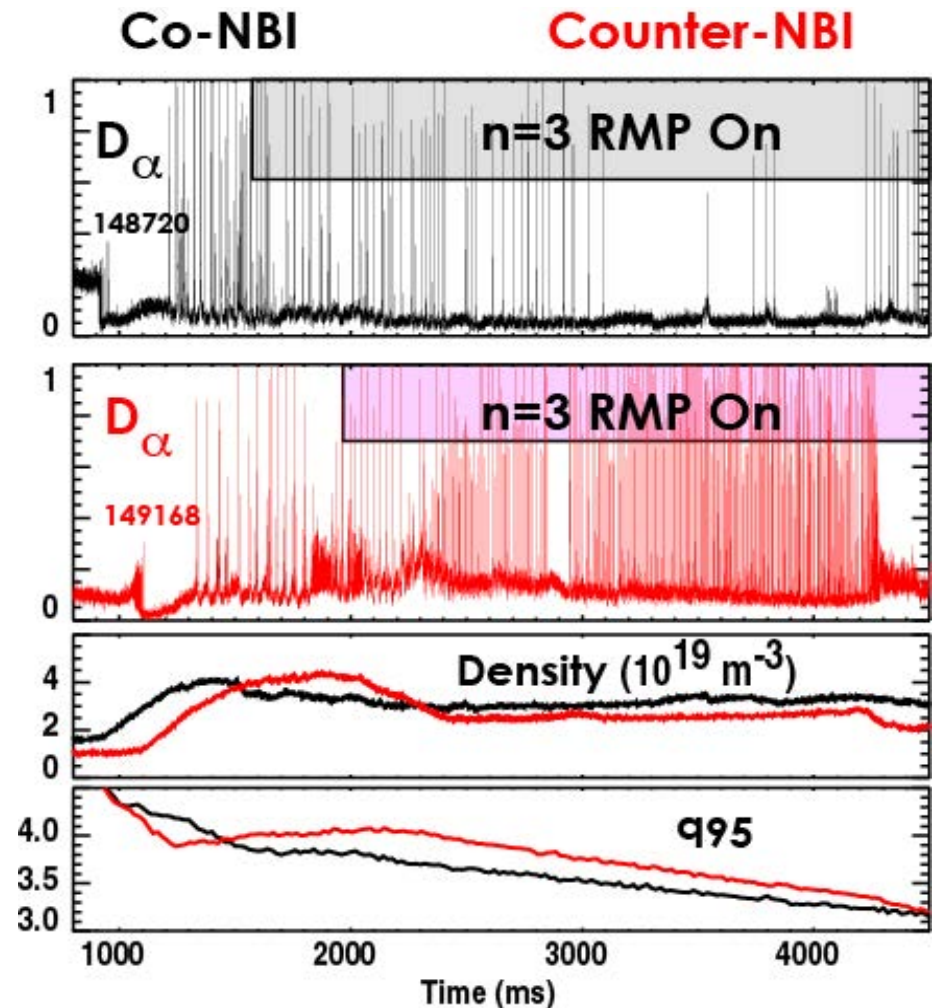
$$\omega_{\perp,e} = \omega_{\text{ExB}} + \omega_{\text{e,dia}}$$

- If MHD response is strongly dependent on $|\omega_{\perp,e}| \approx 0$, should be difficult to obtain ELM suppression with counter NBI



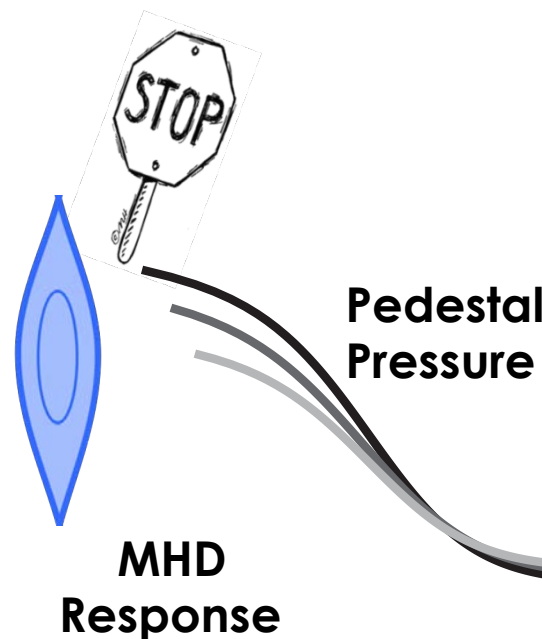
Lack of ELM suppression with Counter-NBI Indicates Importance of $\omega_{\perp,e}$ at Top of Pedestal

- ELMs remain in counter-NBI q_{95} ELM suppression window typically seen with co-NBI
 - Even at comparable density
- Small window of ELM suppression observed at $q_{95} \sim 4.0$
 - EHO signature also observed \rightarrow QH-mode??



Significant Progress Has Been Made in Improving the Physics Basis for RMP ELM Suppression in ITER

- **ELM suppression extended to ITER scenarios**
 - ITER Baseline Scenario
 - Large helium fraction
- **Measurements consistent with emerging model**
 - RMP induces MHD response at top of pedestal
 - Resulting transport impedes further widening of the pedestal
 - Peeling-ballooning stability maintained – No ELMs!!!



Significant Progress Has Been Made in Improving the Physics Basis for RMP ELM Suppression in ITER

- **ELM suppression extended to ITER scenarios**
 - ITER Baseline Scenario
 - Large helium fraction
- **Measurements consistent with emerging model**
 - RMP induces MHD response at top of pedestal
 - Resulting transport impedes further widening of the pedestal
 - Peeling-ballooning stability maintained – No ELMs!!!

Future Plans

- Compatibility with fueling
- Pure helium plasmas
- ...
- Better quantify MHD response across range of conditions
- Connect MHD response to transport modifications